April 1, 2002
TWP: MHECECAEX
MSAD-02-0197

TO: M. Ewert /EC2

VIA: J. Keener /C70

FROM: Gregg Weaver /C70

SUBJECT: Advanced Radiator Concepts and Carbon Velvet Cold Plate Thermal/Vacuum Test Post-Test Report

This report is meant to satisfy the requests outlined in TWP MHECECAE3 relating to the advanced radiator test completed in 2001. The attached document, "Advanced Radiator Concepts and Carbon Velvet Cold Plate Thermal/Vacuum Test Post-Test Report", JSC 47823, is the final report for the corresponding Chamber B test.

Gregg S. Weaver
Environmental Analysis Section

DISTRIBUTION

C. Lin	/EC2	
M. Ewert	/EC2	
K. Hurlbert	/EC2	
C. Cross	/EC2	
D. Westheimer	/EC2	
W. Ruemmele	/EC2	
J. Cox	/C70	
J. Keener	/C70	
G. Weaver	/C70	
T. Durrant	/C70	
K. Stafford	/C70	
T. O. File		
Records Center	/B15	(2)

LOCKHEED MARTIN

April 1, 2002
TWP: MHECECAEX
LMSEAT 33949

ADVANCED RADIATOR CONCEPTS AND CARBON VELVET COLD PLATE THERMAL/VACUUM TEST POST-TEST REPORT

PREPARED BY

Gregg S. Weaver, Analyst
Environmental Analysis Section

APPROVED BY

John F. Keener, Project Manager
Environmental Analysis Section

John L. Cox, Ph.D., Section Manager
Environmental Analysis Section

Lockheed Martin Space Operations
Houston, Texas

CREW AND THERMAL SYSTEMS DIVISION

NASA - LYNDON B. JOHNSON SPACE CENTER

JSC 47823

ADVANCED RADIATOR CONCEPTS AND CARBON VELVET COLD PLATE THERMAL/VACUUM TEST POST-TEST REPORT

DOCUMENT NUMBER	DATE
CTSD-ADV-485	April 1, 2002

PREPARED BY:	**G. S. Weaver**
PREPARED BY:	**D. T. Westheimer**
APPROVED BY:	**C. H. Lin**

No. Of Pages: 61

REVISIONS

REVISION LETTER/DATE	PREPARER	APPROVALS		AUTHORIZED
		BRANCH	PROGRAM	

JSC Form 151C (Apr 91)

Advanced Radiator Concepts and Carbon Velvet Cold Plate Thermal/Vacuum Test Post-Test Report

Gregg S. Weaver
Lockheed Martin Space Operations
Houston, Texas 77058

David T. Westheimer
NASA Johnson Space Center
Houston, Texas 77058

April 1, 2002

Table of Contents

Table of Tables

Table of Figures

Nomenclature

CTSD	Crew and Thermal Systems Division
cm	centimeter
DTP	detailed test procedure
EATCS	External Active Thermal Control System
ESLI	Energy Science Laboratories, Inc.
FLUINT	Fluid Integrator (software)
FMF	Flexible Metal Fabric (Radiator)
GMT	Greenwich Mean Time
hr	hour
in or "	inches
IR	infrared
ISS	International Space Station
JSC	Johnson Space Center
K	Kelvins
kg	kilogram
lbs	pounds
LHP	Loop Heat Pipe and Carbon Fiber Fin (Radiator)
m^2	meters squared
NASA	National Aeronautics and Space Administration
PGW	propylene glycol and water
SINDA	Systems Improved Numerical Differencing Analyzer (software)
TC	thermocouple
TR	test requester
W	Watts

INTRODUCTION

The proper operation of space hardware requires a robust and efficient thermal control system to reject waste heat generated by equipment and crew. Once collected from the source, waste heat that is not intended for reuse must be rejected to space. Radiators are heat rejection devices commonly used on space hardware. Although current radiators are capable of rejecting heat in a variety of space environments, improvements in efficiency, reduction in mass, and improvements in deployment methods are some of the many ways in which engineers are attempting to reduce the overall cost of rejecting heat in space using radiators.

Two advanced radiator designs were recently tested at the Johnson Space Center (JSC) in Houston, Texas. These radiators were originally designed for application on an expandable space vehicle, TransHab, and to employ new features intended to make them more desirable than currently-used technology. One, the Flexible Metal Fabric (FMF) Radiator, is notable because it can roll into a compact shape and then unfurl upon reaching its destination, thus simplifying delivery and deployment of the radiator. The other, the Loop Heat Pipe and Carbon Fiber Fin Radiator, hereafter referred to as the LHP radiator, is also innovative because of its flexibility, and also because it utilizes a loop heat pipe intended to distribute waste heat more efficiently throughout the radiating surface. Both radiator manufacturers also claimed many other advantages over previous technology, including improved reliability, decreased mass, decreased cost, and/or increased efficiency, among others.

The recent test at JSC evaluated the performance of these radiators in a thermal/vacuum chamber designed to simulate applicable space environments. Test data were analyzed to evaluate the heat rejection capabilities of these radiators, and this paper documents the findings of the post-test analysis.

Also tested concurrently with the radiators was the Carbon Velvet Cold Plate test article. Equipment can be cooled through a variety of means, and air-cooling of equipment is common within crew cabins. However, a more cost-effective means of cooling is to employ the use of cold plates. This involves placing a liquid-cooled plate on a hot surface, thereby drawing waste heat into the coolant, as opposed to allowing it to enter the surrounding air. Cold plates can also be used in a vacuum environment to cool equipment. In practice, the liquid coolant ultimately would be transported to heat rejection devices, such as radiators, where it would reject its waste heat.

However, the effectiveness of this technique is dependent upon the thermal conductivity at the interface between the heat producing equipment and the cold plate. As such, the development of materials to improve the heat transfer at this interface is of interest. One such interface material is carbon velvet, and the Carbon Velvet Cold Plate test article, described below, was tested to evaluate the effectiveness of carbon velvet in a vacuum environment[1].

Currently, the cold plates used in the International Space Station (ISS) External Active Thermal Control System (EATCS) have an additional requirement to allow for easy separation of the heat-producing electronics and cold plate. This led to a radiant fin design where the electronics

[1] In this test, the coolant used by the cold plate was not directed to the nearby FMF nor LHP radiators. Each of the three test articles was tested simultaneously, but separately.

are attached to a set of aluminum fins that intermesh with another set of liquid-cooled aluminum fins. This created a thermal interface by radiation between the two sets of fins. The Carbon Velvet Cold Plate test article, which was based on the ISS radiant fin design, utilized a carbon velvet thermal interface that was attached to the fins that were heated by the electronics. Once the sets of aluminum fins are intermeshed, the carbon velvet conformed to fill the space between the two sets of fins, thereby changing the radiation interface into a conduction interface.

This report documents relevant findings from the Carbon Velvet Cold Plate post-test analysis.

Scope

This document provides the results for the thermal/vacuum test of the FMF radiator, the LHP radiator, and the Carbon Velvet Cold Plate test articles. These were tested for the Crew and Thermal Systems Division (CTSD) at JSC, in Chamber B of Building 32, from September 17 through September 23, 2001.

Test Objectives

The test objectives for the radiators, as outlined in their corresponding test plan document [1][2] are as follows:

> The primary objective of this test is to evaluate and compare the performance of two different radiator concepts. The following objectives apply to both test articles:
>
> A.1 Evaluate heat rejection of each radiator during steady state and transient operation.
> A.2 Demonstrate heat rejection capabilities in predicted operating environments.
> A.3 Measure pressure drop across each radiator at different operating flow rates.
> A.4 Confirm flexibility.

The test objective for the carbon velvet cold plate test article, as outlined in its corresponding test plan document [2] is as follows:

> The primary objective of this test is to evaluate the thermal performance of the Carbon Velvet Coldplate in vacuum conditions.

DETAILED TEST ARTICLE DESCRIPTIONS

All three test articles were tested in the Chamber B thermal/vacuum test facility in Building 32 at JSC. The chamber was evacuated and the chamber walls were cooled with liquid nitrogen.

Heaters were used to raise the temperature of the surroundings of the radiator test articles to simulate the environments that they might be expected to see during operation in space.

Mixtures of propylene glycol and water (PGW, 60% propylene glycol and 40% water by mass)

[2] Numbers in brackets correspond to references listed at the end of this document.

provided heat transport to and from all three test articles. Filtrine carts, located outside the chamber, controlled the temperature of the fluid delivered to the test articles[3]. Figure 1 shows the general layout of the test articles in the chamber[4]. As can be seen in Figure 1, one Filtrine cart (#1) serviced the radiators, while another (#5) serviced the cold plate.

Each test article was isolated from the others such that radiation heat transfer between them was negligible. Also, the radiators were plumbed in parallel so as to reduce interactions between them. Thus, although the radiators and cold plate were all tested simultaneously in the same vacuum chamber, the lack of significant interaction between them allowed each test article to be studied separately.

To prevent the lines from freezing, heat traces (resistive heaters) were attached along the tubes connecting the Filtrine carts to the test articles. Insulation was wrapped around the outside of the heat trace/tube combination to reduce heat loss. Nominal operation did not call for the use of the

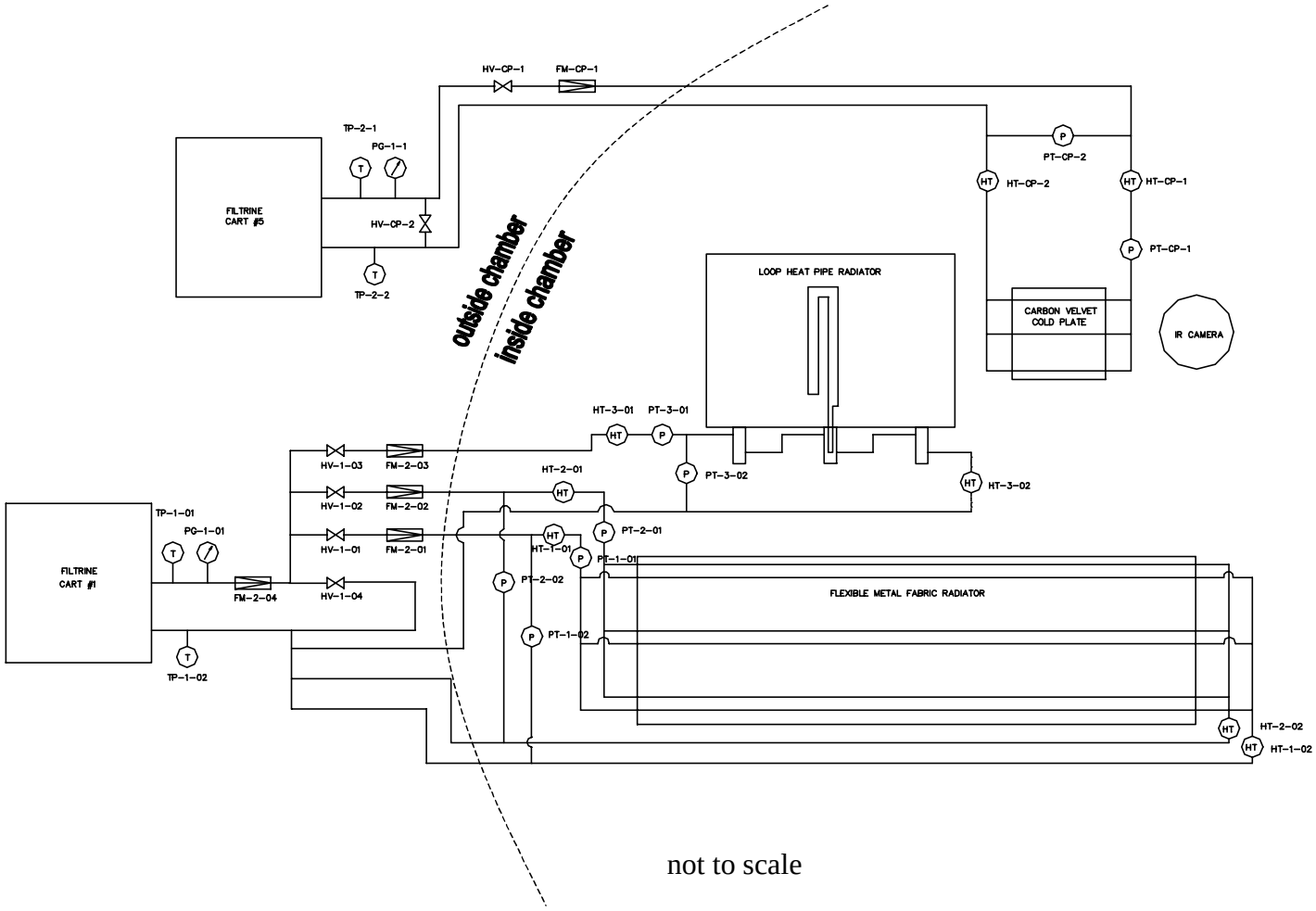

not to scale

Figure 1 - Test Chamber Layout

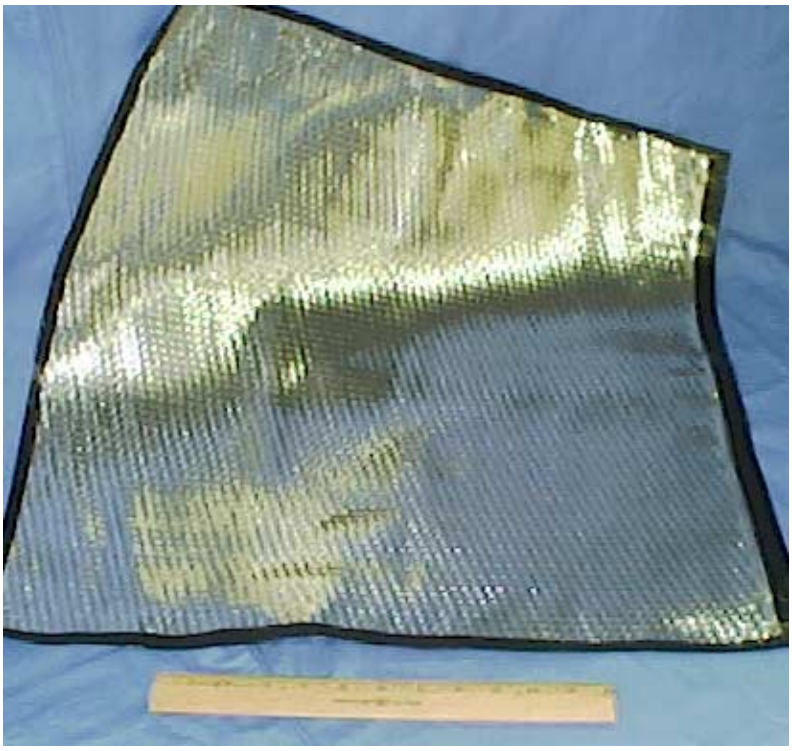

Figure 2 - FMF Flexibility

heat traces; they were installed for contingency response.

An infrared (IR) camera (seen in Figure 1), was used during the test to study the test articles.

The radiators were designed to have a mass per area of less than 3.7 kg/m^2, which is an improvement over the ISS radiator mass of 8.5 kg/m^2. They were also designed to radiate 170 W/m^2 at an environment temperature of 155 K, with a radiator inlet temperature of 291 K.

Flexible Metal Fabric Radiator

The FMF radiator, designed at JSC, was comprised of aluminum strips woven together by Prodesco[5] and bonded[3] to stainless steel tubes by Materials Resources International[6]. The stainless steel tubes were attached to flexible manifolds, located at both ends of the radiator. Two separate PGW loops serviced the radiator, Loop A and Loop B. Thus, there were two inlet manifolds and two outlet manifolds. During the Chamber B test, PGW entered the "north" manifolds, flowed through the tubes, and exited the "south" manifolds. The woven aluminum and the flow tubes were painted at JSC with Chemglaze A276, yielding an emissivity, ε=0.89[4]. The radiating surface area was 4.56 m by 1.09 m (4.98 m^2).

The flexibility of the woven aluminum can be seen on the material sample shown in Figure 2. Measuring the flexibility of the radiator was a test objective, and results are documented later in this paper. The painted test article can be seen in Figure 3. A flexible manifold, made of a stainless steel bellows-style flex hose, is pictured in Figure 4 and in Figure 5. The flow tubes can be seen in Figure 5 as well, as small tubes attached to the manifolds.

The FMF radiator was positioned horizontally in Chamber B, as shown in Figure 1. It was supported by an aluminum table. NOMEX® insulation and a layer of Mylar® were inserted between the table and the radiator to prevent heat transfer out the bottom of the radiator. The table was supported by Teflon® blocks (see Figure 6).

[3] The S-bond™ technique was used.
[4] The emissivity of the FMF radiating surface was measured at 3 locations after the test. Emissivity values of 0.88, 0.89, and 0.90 were measured.

Figure 3 - Painted FMF Radiator

A "heater cage" was constructed above the radiator. It was composed of heater bars arranged horizontally 23 inches above the radiator. Each heater bar was 31.5 inches long, 1.5 inches wide, and 0.5 inches thick. Heaters were spaced 3 inches apart and were arranged, qualitatively, as shown in Figure 7. The end of each heater was attached to an aluminum support (not shown in the figure). The heater cage concept was used instead of traditional IR lamps because the concept has been shown to provide a uniform thermal environment, even when variations in surface optical properties are present [7]. The power to the heaters was variable during the test such that a wide range of thermal conditions could be produced. Mylar® (also shown in Figure 7) was hung vertically around the test article to prevent radiation exchange with the other test articles. The perimeter of the Mylar® was larger than the perimeter of the radiator, so a gap was present around the edge of the radiator. A pre-test analysis showed that such a gap would yield more uniform surface temperatures. A summary of the pre-test analyses can be found in [8].

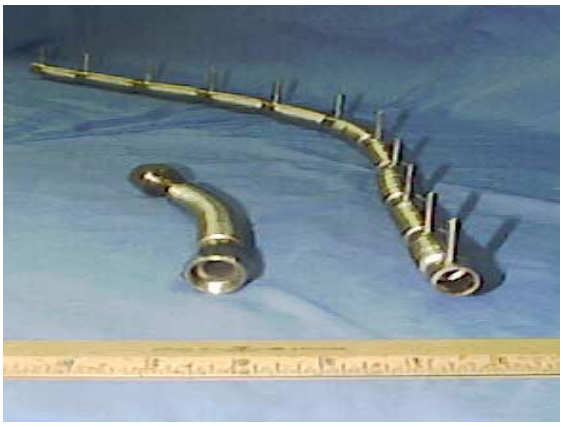

Figure 4 - FMF Manifold

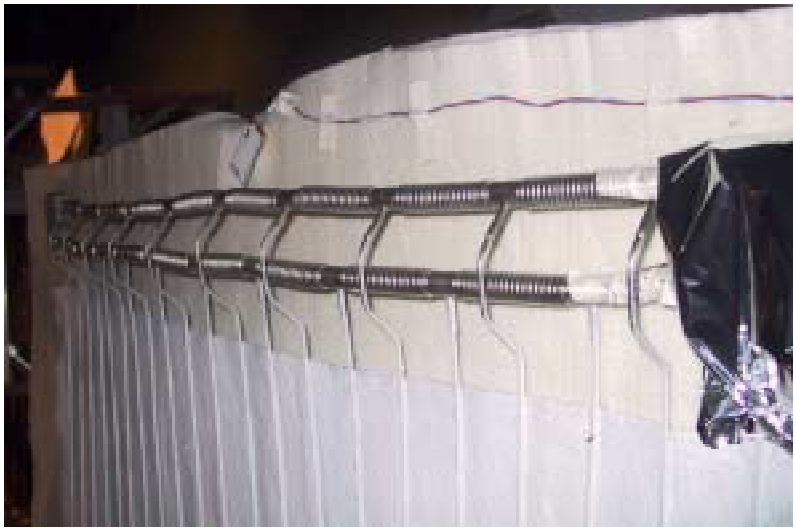

Figure 5 - FMF Manifold Installed

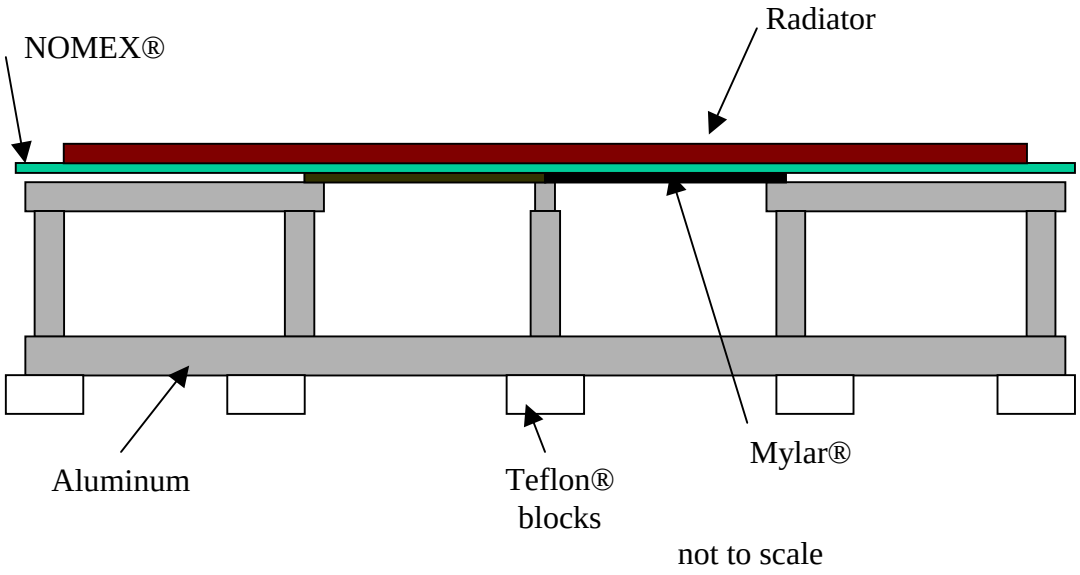

Figure 6 - FMF Arrangement

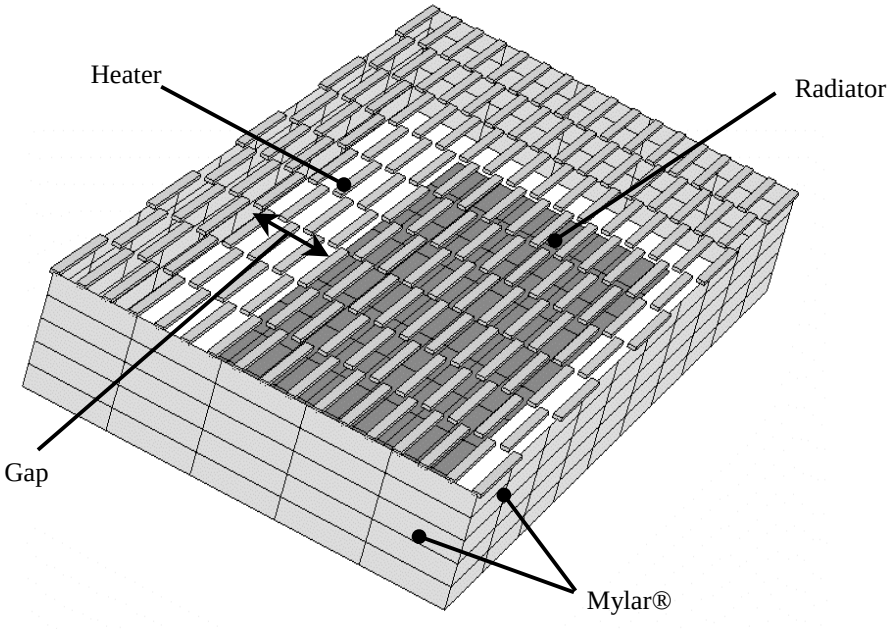

Figure 7 - Heater Cage Setup

Loop Heat Pipe Radiator

The LHP radiator was positioned in Chamber B as shown in Figure 1. The radiator was designed and manufactured by Lockheed Martin Missiles and Fire Control in Dallas, TX. The PGW flowed from the Filtrine cart to a series of copper powder heat exchangers located along the "west" side of the radiator. These heat exchangers were designed to transfer heat from the PGW to loop heat pipes attached along the underside of the radiator (refer to Figure 8). The loop heat pipes were designed to then spread the heat acquired from the PGW (via the heat exchangers) throughout the surface of the radiator. Figure 9 shows a cross section of one of the circular heat pipes; it is embedded in the middle of an aluminum extrusion[9]. The cross-section of the radiator panel was made of woven carbon fiber fabric, to help spread heat from the loop heat pipe uniformly throughout the radiating surface. Sheets of Mylar® were bonded to both sides of the woven carbon fiber fabric. The loop heat pipes and copper powder heat exchanger were designed and manufactured by Thermacore, Inc.[10].

The radiating surface area was 0.86 m by 1.85 m (1.60 m^2). The surface of the radiator was covered with a supposedly-flexible Z-93 thermal coating; however, parts of the coating flaked off to expose bare Mylar®. Flaking occurred when the radiator was flexed. Figure 10 shows the original test article, and Figure 11 shows the appearance of the radiator after it had been installed in Chamber B. A prototype radiator coated with the flexible Z-93 coating did not suffer from flaking when flexed; the cause for the flaking here was not determined.

In the chamber B test, 3 heat exchangers were used; these can be seen at the top of Figure 10. However, only the center heat exchanger interfaced with a working loop heat pipe, which was charged with ammonia. The other 2 loop heat pipes were not charged before the test and were not functioning. The "south" non-functioning loop heat pipe is called "Dummy 1", and the "north" non-functioning loop heat pipe is called "Dummy 2".

To simulate the performance of a loop heat pipe, Minco® strip heaters were placed along the aluminum extrusions containing the non-working loop heat pipes[11]. Five or six heaters, depending on the length of the extrusion, were placed on alternating sides of the uncharged loop heat pipe. Heater dimensions were 0.27 inches by 5.5 inches. They were spaced uniformly along the extrusions; however, heater locations were not identical for each extrusion because, at several locations, foreign material had adhered to the surface and interfered with heater placement. Figure 12 illustrates how these heaters were placed on the test article.

The power to the Minco® heaters could be regulated, and the detailed test procedure (DTP) called for these heaters to be controlled during the test such that the surrounding radiator surface temperatures approximated those near the working loop heat pipe[12].

As with the FMF radiator, the thermal environment surrounding the LHP radiator was controlled with heater bars, and the test article was surrounded by Mylar®, as shown in Figure 7. Each heater bar was 23.5" long, 1.5" wide, and 0.5" thick, and the heater cage was 21.5" above the radiator surface.

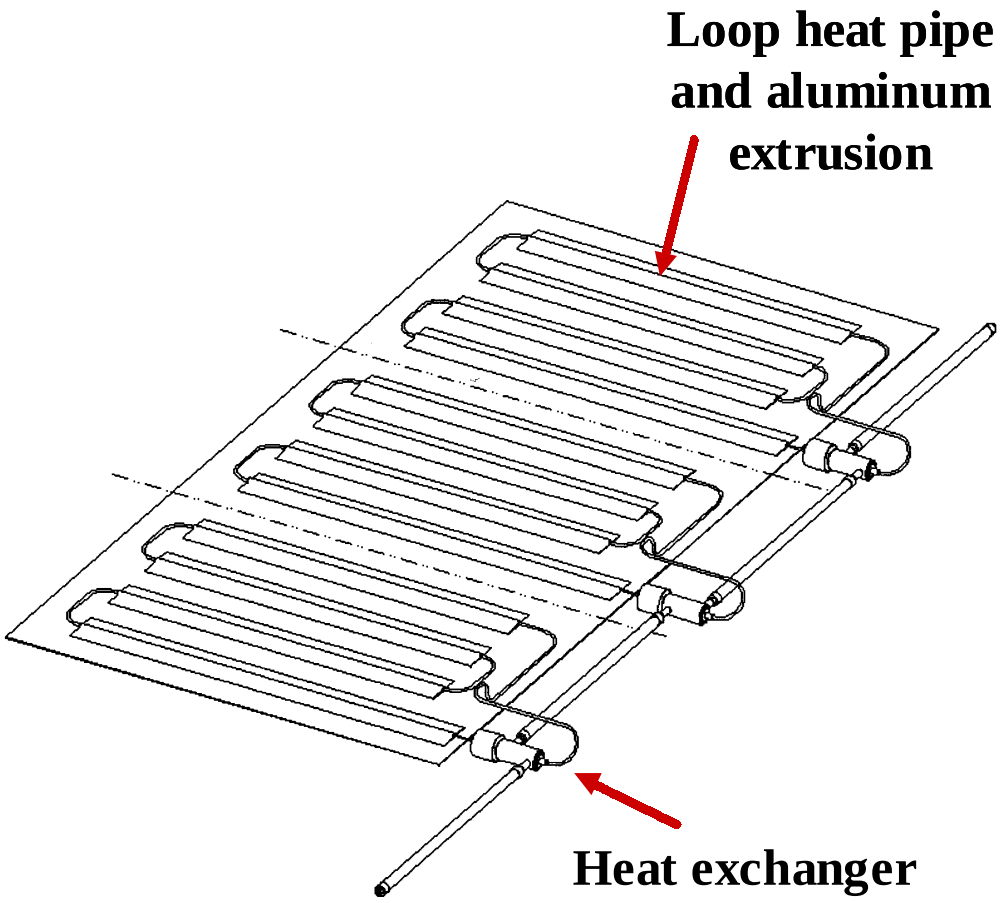

Figure 8 - Loop Heat Pipes and Heat Exchangers

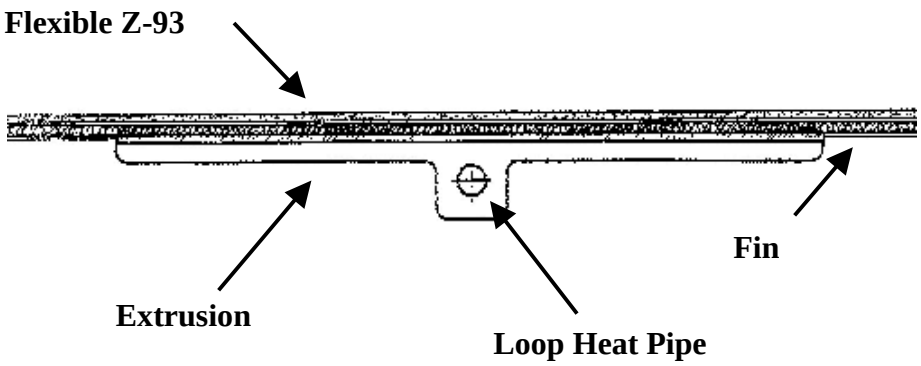

Figure 9 - Loop Heat Pipe Cross-Section

Figure 10 - LHP (When Received New)

Figure 11 - LHP Flaking

The emissivity of the Z-93 was measured in 3 radiator surface locations after the test[5] and was found to average ε=0.90. The exposed Mylar® was found to have an emissivity of ε=0.72. For use in calculations, an emissivity of 0.90 was assumed.

The LHP radiator was positioned horizontally in Chamber B, as shown in Figure 13. It was supported by an aluminum table. NOMEX® insulation was inserted between the radiator and the table to prevent conduction heat transfer. Teflon® blocks also reduced heat transfer out the bottom of the radiator. Unlike in the FMF radiator setup (Figure 6), Mylar® was not placed below the radiator[6].

[5] Measurements were 0.89, 0.91, and 0.89.
[6] Mylar® was not needed since the LHP table did not contain gaps. (Gaps would have increased the likelihood of radiation out the bottom of the radiator.)

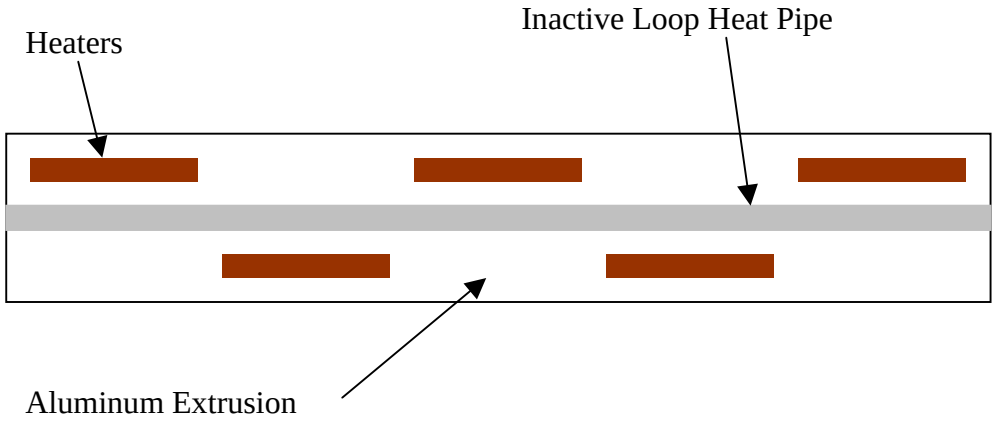

Figure 12 - Heater Placement to Simulate Loop Heat Pipe

Carbon Velvet Cold Plate

Carbon velvet material was designed by Energy Science Laboratories, Inc. to enhance heat transfer across thermal interfaces[13]. It was developed for use with heat acquisition hardware, including the ISS cold plate. In theory, the heat flux can be greatly increased for an existing footprint and temperature range, which could, for example, accommodate more powerful avionics.

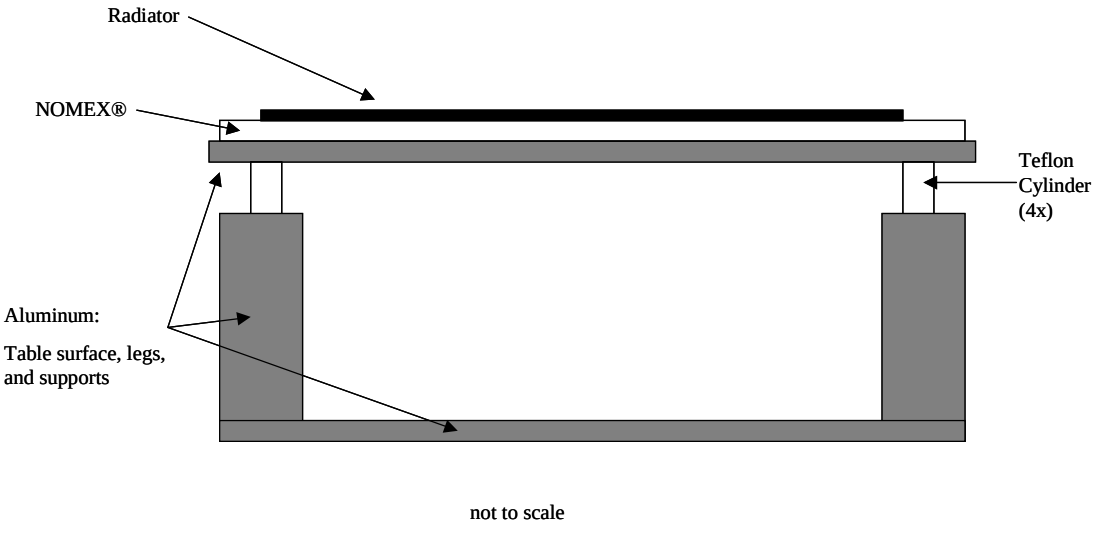

Figure 13 - LHP Arrangement

Figure 14 - Carbon Velvet Cold Plate Test Article

The Carbon Velvet Cold Plate was tested to determine the efficiency of carbon velvet material. Figure 14 is a picture of the test article prior to the test. The cold plate was 53 cm x 55 cm and approximately 45.5 kg (100 lbs). It consisted of three components bolted to a mounting plate: a set of radiant fins with carbon velvet on the fins and heaters mounted on the top surface; another set of radiant fins; and a cold plate that had flow passages, which provided cooling to the assembly. Dow Corning 340 silicone heat sink compound was used for the thermal interface between the bottom set of radiant fins and the cold plate.

Figure 15 shows the components that make up the Carbon Velvet Cold Plate test article. Entrance and exit manifolds for the PGW are on either side of the cold plate. Minco® electrical heaters were attached to the top of the article (shown as rows of rectangles in Figure 16) to

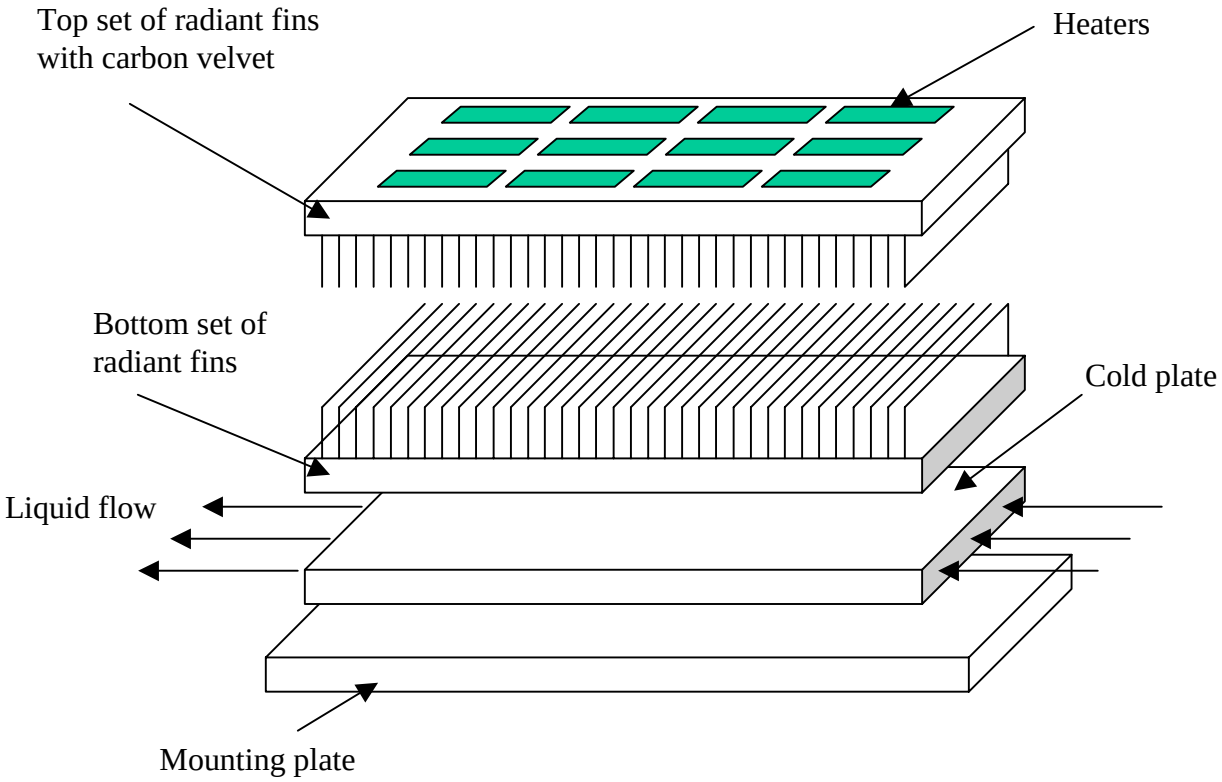

Figure 15 - Cold Plate Components

simulate heat-producing electronics. The two sets of radiant fins mesh together as shown in Figure 17, and a sample of carbon velvet material can be seen in Figure 18.

The cold plate was designed to simulate a DC-DC Control Unit Cold Plate for use on the ISS EATCS. This application requires that the cold plate assembly reject 694 W with a coolant flow rate of 125 lbm/hr and an inlet temperature of 39 °F[14]. This test condition and a similar test condition with an inlet temperature of 63 °F, another common ISS coolant temperature, were run to directly compare the performance of this enhanced cold plate to the ISS specification. It should be noted that the ISS EATCS uses ammonia as a coolant and this test used a propylene-glycol and water mixture.

If the carbon velvet were not used, energy from the heaters would radiate from one set of fins to the other, and then be removed at the bottom by the PGW. The addition of the carbon fiber material between the fins was expected to increase the heat transfer rate by replacing the radiation mechanism with conduction between the fins. The carbon velvet was placed on the top set of fins only.
controllability

The cold plate was located in the chamber as shown in Figure 1, and it was serviced by its own Filtrine cart. It was insulated from the environment, as the purpose of this test was to determine performance in a vacuum, without regard to the surrounding temperatures.

INSTRUMENTATION

Thermocouples, temperature probes, flow meters, pressure transducers, and delta pressure transducers were used in the test to verify that the desired test points had been attained, to ensure the safety of the equipment, and to evaluate the performance of each of the test articles.

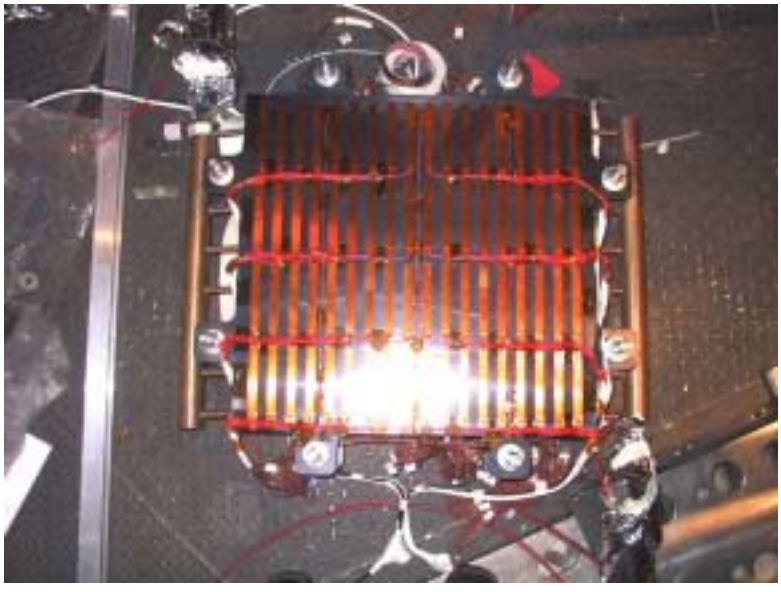

Figure 16 - Cold Plate Minco® Heaters

General

Figure 1 shows the locations of instruments along the fluid lines leading to and from each test article. Appendix A contains additional instrumentation figures.

To summarize the instruments in Figure 1, temperatures were measured upstream and downstream of each Filtrine cart as well as upstream and downstream of each test article. The absolute pressure was measured at the entrance of each test article (to

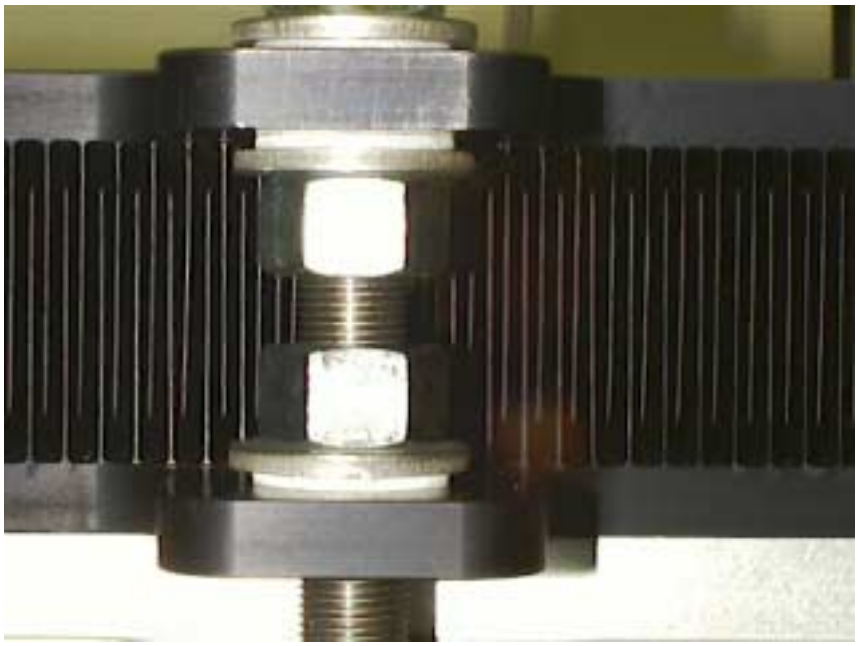

Figure 17 - Cold Plate Fins

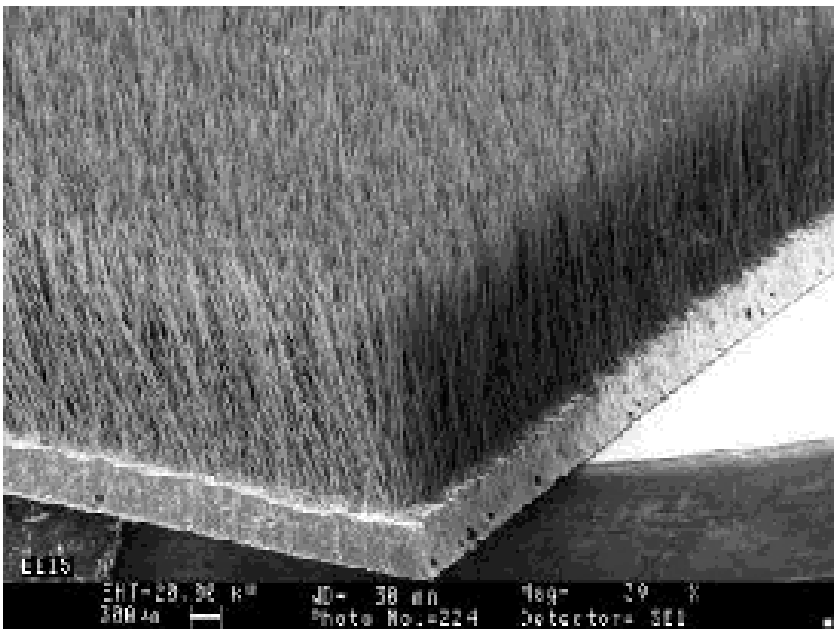

Figure 18 - Carbon Velvet Fibers

help ensure that the pressure did not exceed the tolerance of the equipment), and the pressure difference across each test article was measured. The flow rate exiting each Filtrine cart was measured, and the flow rate leading to each test article was measured as well. Also shown in Figure 1 are the locations of the hand valves used to regulate the flow to each of the test articles. Note that "TP" and "HT" refer to temperature measurements, "PT" refers to pressure measurements, and "FM" refers to flow rate measurements.

Flexible Metal Fabric Radiator

Figure 19 shows the locations of the thermocouples on the FMF radiator[4]. All of the thermocouples were placed on the underside of the radiating surface so as not to interfere with the radiation process.

In summary, thermocouples 1 through 30 were placed directly opposite of the tubes along the length of the radiator (the tubes were on the top of the radiator, while the TCs were underneath the radiator.) Half of the TCs were placed on Loop A, while half were placed on Loop B. Note that 22 flow tubes serviced

the FMF radiator (11 on each loop), but only 6 are shown in Figure 19. The other loops were not instrumented. If the tubes were numbered from 1 through 22, with "1" being on the east side, then the tubes that were instrumented were tubes 1, 2, 11, 12, 21, and 22.

Additionally, thermocouples 31 through 58 were placed on the woven aluminum material, perpendicular to the flow tubes. These thermocouples were meant to determine the temperature distribution between the flow tubes. They were spaced 1.6 cm apart and centered on a tube. They were placed on the aluminum strips transverse to the tubes. Thermocouples 31 through 37 were placed 38 cm from the north end; thermocouples 38 through 44 were placed 42 cm from the north end, thermocouples 45 through 51 were placed 41 cm from the south end; and thermocouples 52 through 58 were placed 33 cm from the south end. The lowest-numbered thermocouple in each set was placed closest to the manlock (on the west side).

More details as to the placement of the thermocouples can be found in Figure 36 in Appendix A.

Finally, "coupons" were used to measure the environment at 4 locations. They are indicated by shaded squares in Figure 19 and are labeled TTB 341, 342, 343, and 345. The PCC labels correspond to different heater cage "zones" (marked by dashed lines) that could be controlled independently. Each coupon was a small piece of aluminum that was painted with Z-93 on one side. A thermocouple was placed on the unpainted side, which was then covered with a piece of Mylar®. The coupon was placed on the sheet of NOMEX® (which was insulating the table from the radiator) with the painted side pointed up.

Loop Heat Pipe Radiator

Figure 20 shows the locations of the thermocouples on the LHP radiator. All of the thermocouples were placed on the underside of the radiator so as not to interfere with the radiation process.

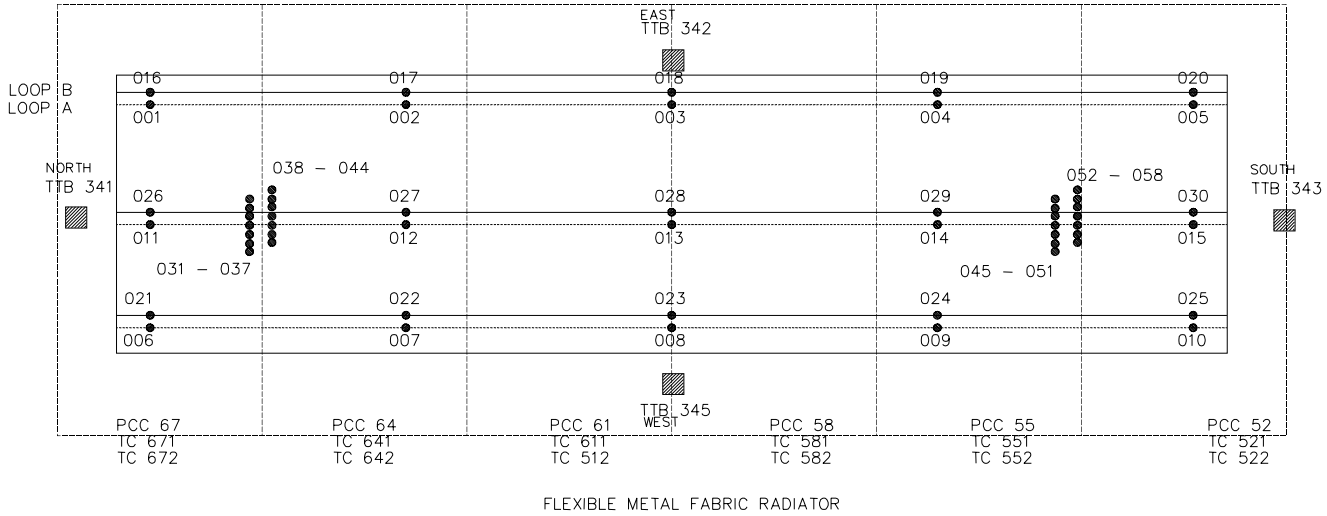

Figure 19 - FMF Instrumentation

Thermocouples 4 through 16 were placed on the outer surface of the working loop heat pipe. Thermocouples 22 through 33 and thermocouples 39 through 50 were placed on the non-working loop heat pipes in the vicinity of the Minco® heaters. Other thermocouples (e.g., 1, 2, 3, and 17) were placed on or near the heat exchangers. Thermocouples 52 through 63 were placed on the aluminum extrusions at a location near the center of the radiator. Thermocouples 64 through 67 were placed directly on the radiator. Finally, thermocouples 68 through 80 and thermocouples 88 through 99 were placed perpendicular to the loop heat pipes on the extrusions and on the radiator to ascertain the temperature distribution between the pipes.

More details as to the placement of the LHP thermocouples can be found in Appendix A.

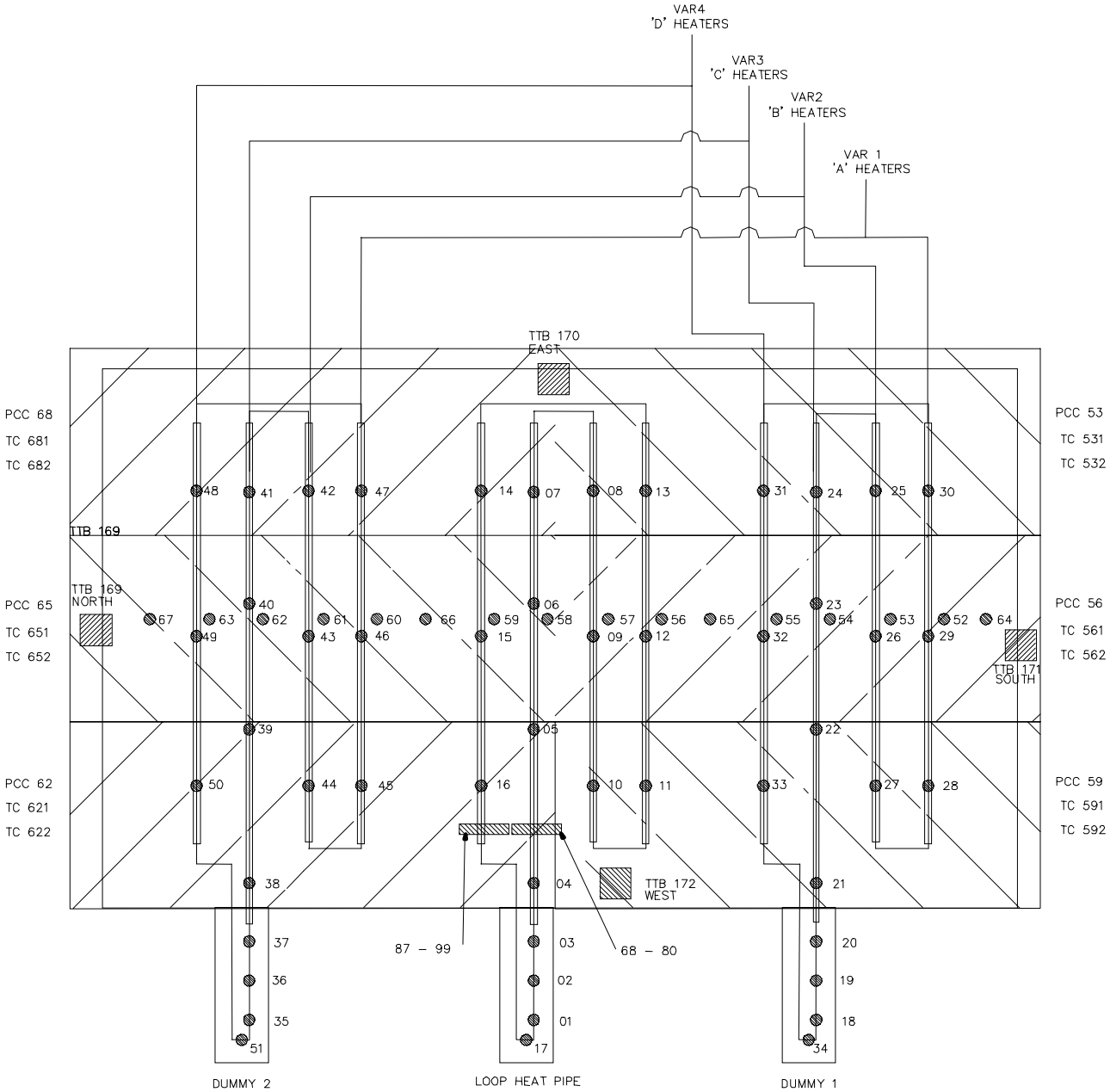

Figure 20 - LHP Instrumentation

In addition to the thermocouples, 4 coupons were placed next to the radiator to determine the environment temperatures. These are indicated by shaded squares on Figure 20, and they are labeled TTB 169, 170, 171, and 172. Their construction was the same as for those used to measure the FMF radiator environment.

Figure 20 also indicates how the Minco® heaters were wired. They were divided into 4 groups, Heaters A, B, C, and D. These were controlled by Variac controllers 1, 2, 3, and 4, respectively. These Variacs could be set independently during the test to warm the radiator surface near the non-functioning loop heat pipes.

Carbon Velvet Cold Plate

Thermocouples were installed on the Carbon Velvet Cold Plate to determine the temperature difference between each layer of the cold plate assembly and to verify that the temperatures were uniform on each component. Figure 21 shows how these surface-mounted thermocouples were located on each component of the cold plate. Thermocouple spacing was the same for each component of the cold plate assembly. TCs 001 – 009 were mounted on the top surface of the top set of radiant fins, TCs 010 – 018 were between the fins on the base of the top set of radiant fins (with the carbon velvet), TCs 019 – 027 were between the fins on the base of the bottom set of radiant fins, and TCs 028 – 036 were on the bottom of the cold plate.

Thermocouples were numbered from the lower left hand corner of Figure 21 with the numbers increasing to the right and then to the row above.

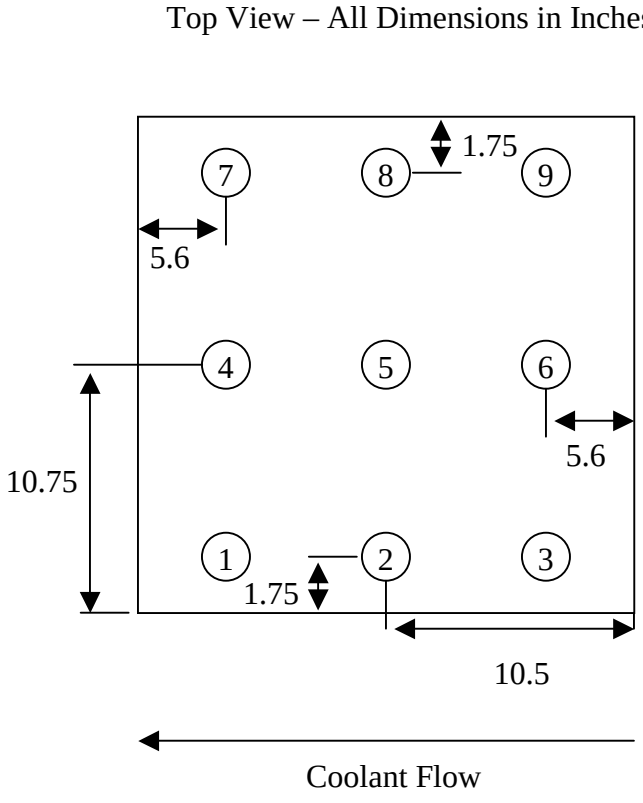

Figure 21 - Cold Plate Thermocouple Numbering (Top View)

Discrepancies

The IR camera worked correctly, producing color pictures, at the beginning of the test. It failed, however, during the middle of the test. It was determined that the problem was in the wiring between the camera and the control room. This was partially fixed, allowing for black-and-white images (as opposed to color) for the remainder of the test.

Many of the voltage and power readings in DARS were off by a factor of two. Post-test, it was necessary to adjust the data for PCCs 56, 59, 62, 65, and 68 by multiplying all

of the values by two. These PCCs controlled the heaters above the LHP radiator.

Also, the power reading on PCC 71, which output the power to the cold plate heaters, was off by a factor of two for a large portion of the test. This problem was noted during the test and corrected. However, all PCC 71 power data before the fix was implemented (GMT 263-15:09) had to be adjusted post-test by multiplying the recorded values by two.

There was a concern over the temperature measurements at the inlet and outlet of the cold plate (HT-CP-01 and 02). During periods of time with no heat load to the cold plate, a temperature increase from inlet to outlet of up to 0.4°F was often observed. However, it was not always present. Probable explanations include instrument error or interaction with the heat trace on the cold plate fluid lines. This temperature increase corresponds to 104 W at the 1100 lbm/hr flow rate (the flow rate at which most of the cold plate test points were run).

TC-CP-11 appeared to give erroneous readings occasionally during the test. Recorded temperatures were approximately 100°F hotter than nearby temperature measurements and had a large scatter. This behavior appears to have only affected data for Test Points 41, 51, and 52.

TEST SUMMARY

The general test procedures are outlined in the DTP. However, some deviations to the DTP were made during the test to accommodate unexpected test article behavior. The baseline procedures and the deviations are discussed below.

Baseline Plan

The DTP outlines the baseline test procedures. It called for testing the LHP and FMF radiators at 39 test points each, and the cold plate at 16 test points.

In summary, the radiator environment temperatures were to be set to -240°F, -180°F, -25.6°F, and 27°F. At each environment, the radiator inlet temperatures were to be set at specified conditions ranging from 37°F to 135°F. Also, the flow rates to each radiator were to be varied from 50 to 500 lb/hr.

Steady state for the radiators was determined when changes in certain critical temperatures were constant within 1°F for a thirty minute period. Specifically, outlet temperatures for both radiators were monitored (FMF: HT-1-02 and HT-2-02, for Loops A and B, respectively; LHP: HT-3-02) as well as calculated surface temperature averages (LOOPAB for the FMF and LOOPHP for the LHP).

The cold plate was thermally insulated from the chamber but was exposed to the vacuum environment. The heater power, inlet temperature, and flow rate were varied during the test.

In addition to simulating predicted operating conditions of the cold plate, the test plan included a series of steps to determine an upper limit for heat transfer performance. An elevated flow rate of 1100 lb/hr was used with both 39°F and 63°F inlet temperatures. The heater power was then

increased incrementally to determine the maximum heat load transferred while maintaining the top surface of the cold plate below 100°F. A temperature of 100°F was chosen as a commonly-accepted temperature limit for electronics cooled by a cold plate.

Steady state for a cold plate test point was defined as a change of less than 1°F over a period of thirty minutes for both the outlet temperature and for the average of the thermocouples mounted on the heating surface of the cold plate. These were calculated in DARS (the data acquisition system) under the name CPHEAT; CPHEAT only included TCs 001 – 007. TCs 008 and 009, which were also on the top surface of the cold plate, were not included because the data acquisition system could only average seven parameters at a time.

Each DTP test point is listed in Appendix B. However, not all of these test points were completed, and some were modified during the test. These modifications are discussed below.

Deviations from the Baseline Plan

Issues arose during the test that prompted modifications to the baseline plan. Refer to Appendix C for a complete listing of the completed, as-modified test points. Notable modifications to the baseline plan are discussed below.

Dummy Heater Settings

The Minco® heaters attached to the LHP radiator were intended to generate a temperature distribution in the vicinity of the non-working heat pipes similar to the temperature distribution produced by the working heat pipe. As shown in Figure 20, the non-working heat pipes are sometimes referred to as "Dummy Loop Heat Pipe #1" and "Dummy Loop Heat Pipe #2". The set of heaters near each of these heat pipes are sometimes referred to as "Dummy Heater #1" and "Dummy Heater #2". Prior to each LHP test point, the test requester (TR) was, according to the DTP, supposed to use the thermocouple data to verify that the Dummy Heaters were set to produce the appropriate temperature distribution[7]. Specifically, TCs 56, 57, 58, and 59 along the working loop heat pipe were supposed to be equal to TCs 52, 53, 54, and 55 along Dummy #1, respectively, and TCs 56, 57, 58, and 59 were supposed to be equal to TCs 60, 61, 62, and 63 along Dummy #2, respectively[8]. A tolerance of ±3°F was acceptable.

However, it was discovered during the test that the heaters were limited to approximately 27% of the available power due to electrical current restrictions on the wires leading to the heaters. As a result, on the test points in which the loop heat pipe reached its hottest temperatures, the Dummy Heaters were not able to generate enough heat, and TRs were forced to accept colder-than-desired Dummy Loop Heat Pipe temperatures.

Note that the Dummy Heaters were intentionally turned off for Cases 10, 11, 21, 22. The Dummy Heater zones were, therefore, much colder than the loop heat pipe zone for these cases.

[7] Test requesters for this test included David Westheimer/JSC, Cindy Cross/JSC, Eugene Ungar/JSC, Gregg Weaver/LMSO, and Kristin Stafford/LMSO.

[8] The DTP actually states that TC's 60, 61, 62, and 63 correspond to Dummy #1, and that TC's 52, 53, 54, and 55 correspond to Dummy #2. This was an error in the DTP.

In addition to the power limitation problem, TC 55 did not work during the test, and TC 56 worked intermittently. This limited the ability of the TRs to accurately set the heaters, and TRs were forced to estimate the missing temperatures based on engineering judgement.

Refer to Table 1 for a summary of the working TCs and Variacs. Aside from Variac 4, which affected only TC 63, note that each of the 4 Variac circuits affected two thermocouple readings that were used for control.

Table 1 - LHP Dummy Heater Characteristics

Heater Zone	Affected These TCs	Set Point Temperature
Variac 1	60, 52	TC 56 (intermittent)
Variac 2	61, 53	TC 57
Variac 3	62, 54	TC 58
Variac 4	63	TC 59

Since there was not a separate heater for each thermocouple, there were some instances in which it was not possible to accurately balance the temperature distributions. With Case 32, for example, TC's 58 and 62 each registered approximately 48°F, while TC 54 registered approximately 55°F. Since both TC 62 and 54 were affected by the same Variac, reducing the power to the Variac could have brought TC 54 into alignment with TC 58, but doing so would have overcooled TC 62. Thus, it was not possible to reach the desired temperatures for both TCs at the same time.

Test data confirm that this problem was uncommon and usually of short duration for the thermocouples affected by Variacs 1 and 2. That is, generally, the TC temperatures on these circuits were similar to each other. Thermocouples 62 and 54 along Variac 3 tended to show a greater temperature spread, and this phenomenon did introduce a limit to how well the DTP requirements could be met. Variac 4 did not exhibit this problem because only one of the TCs was working.

Because of the temperature spread between TCs that were supposed to register the same temperatures, the ±3°F tolerance was generally disregarded during the test, and TRs had the discretion to bring the Dummy temperatures in line with the loop heat pipe temperatures to the best of his or her ability. In some cases, the TR successfully matched the Dummy temperatures to those of the loop heat pipe (e.g., Cases 31 and 32), whereas in others, the TR failed to produce the appropriate temperature distributions. In all cases, however, radiator performance could still be determined for whatever conditions the TR established.

Control of the Environment

The DTP called for testing each radiator at environment temperatures of -240°F, -180°F, -25.6°F, and 27°F. After activating the chamber cold walls, environmental temperatures started falling, but they soon began to level off at temperatures higher than those planned. The DTP was then modified to test the radiators at 4 new, warmer conditions. As can be seen in Appendix C, the

amended LHP radiator environmental set point temperatures were -105°F, -65°F, -45°F, 10°F, and 45°F. The amended FMF radiator environmental set point temperatures were -70°F, -65°F, -45°F, 10°F, and 45°F.

For the coldest test points, the heater cage was left off. Otherwise, the TR attempted to control the environmental temperatures with the use of the heater cages. This was difficult because the 4 coupons did not report similar results. Also, factors other than the heater cage power setting, such as the radiator inlet temperature, affected the coupon readings. Because of the difficulties in setting an exact environmental temperature, the desired tolerance of ±10°F was largely ignored.

Control of the environment was done in the following manner: For each first attempt at setting a new environment, the TR was at his or her discretion to achieve an average environmental temperature close to the new set points. The heater cage settings were recorded, and these heater settings were used for all test points requiring that environmental condition. The heater cage power settings were not adjusted again until a new environmental temperature was desired, and the environment, as measured by the coupons, was allowed to drift according to other influences. This accounts for a discrepancy between the desired environmental conditions and those actually achieved during the test.

Additional Test Point

Test point "35.5" was added to the DTP during the test. This studied both radiators at the following conditions: 45°F environment, 100°F inlet temperature, and 500 lb/hr flow rate.

Test Point Sequence

The test points were not done in sequential order. Since the conditions at each test point were a series of steady state cases, as opposed to a set of points ordered into a transient run, the order in which they were conducted should have had no effect on the results. There were three main reasons the test points were conducted out of order.

It was discovered early in the test that freezing of the PGW was occurring in the FMF for the low flow cases. Rather than consume valuable test time attempting points that might be impossible to achieve, these test points were delayed and, time permitting, attempted at the end of the test after the other test points. As a result, many of the 50 lb/hr test points were not completed because of time constraints. Some of the single-loop cases were not run for this reason as well. (When only 1 loop was running, the FMF was found to freeze in some conditions.)

Another reason the test points were run out of order was to simplify the transition from one test point to another. Changing the conditions of a test point was often time-consuming because of the transients in the system, and it was a quicker process when only one condition was changed between test points, as opposed to changing all conditions every time. For example, Test Point 29 for the FMF called for a 10°F environment, a 135°F inlet temperature, and a 500 lb/hr flow rate. The next case in the DTP, Test Point 30, called for changing all of these conditions (to 45°F, 37°F, and 50 lb/hr, respectively). It was more logical to proceed instead to Test Point 39,

which called for changing only the environment temperature. (Test Point 39 conditions were 45°F, 135°F, and 500 lb/hr.)

The third reason the test points were run out of order was because of problems with the Filtrine chiller cart. For simplicity, LHP and FMF test points were generally run at the same time. However, the Filtrine cart had trouble maintaining a high flow of 500 lb/hr to both radiators simultaneously. Thus, the test points were sometimes run out of order to ensure that one radiator was running at a low flow while the other was running at a high flow.

Radiator Inlet Temperatures

The inlet temperatures for the FMF radiator were increased from 65°F to 100°F for Test Points 21 and 22. This was done to decrease the likelihood of freezing within the radiator.

Sink Temperature Evaluation

Several "sink temperature evaluation" experiments were performed during the test. These test points were created to help the TRs understand the difficulties encountered while attempting to control the radiation environments experienced by the radiator test articles. Sink temperature was defined as the steady state temperature of an adiabatic object in a given environment. Therefore, during these experiments, the flow to the radiators was stopped to eliminate heat transfer with the test article except for radiation. As the radiators came to steady state, the radiator temperatures were compared with the temperatures on the coupons. This was intended to provide the TRs information relating the radiation environment, radiator temperatures, and the coupon temperatures. Results from this experiment were inconclusive.

Transient Cases

The Advanced Radiator Concepts Thermal/Vacuum Test TRD listed the following objective:

> "Evaluate heat rejection of each radiator during steady state and transient operation." [1]

However, it was later decided not to run any transient test points, due to time constraints and because of the low-priority nature of these test points. If specific information on the transient performance of the radiators is desired at a later time, changes between steady state test points can be analyzed or used to validate a transient model.

Cold Plate Deviations

When the heat loads were increased to find the heat load limit corresponding to a 100°F surface temperature, it was determined that all of the planned heat loads would have resulted in surface temperatures above 100°F. As such, most of the cold plate DTP test points were abandoned, and the test team decided to decrease the heater power applied to the cold plate in order to find the heat load that resulted in a 100°F surface temperature for each of the planned inlet temperatures (39°F and 63°F).

SUMMARY OF RESULTS

A summary of the results for the radiators and Carbon Velvet Cold Plate is included below.

Flexible Metal Fabric Radiator Results

As stated earlier, and as can be seen in Appendix C, most of the FMF test points were completed successfully, albeit with modifications to the environment temperature requirements. Heat rejection was evaluated at these test points. Additionally, pressure drop was determined at different operating flow rates, and the flexibility of the radiator was confirmed. Prior to the test, the mass per radiating area of the FMF radiator was found to be 3.4 kg/m^2 (not including the mass of any coolant in the system). This section gives an overview and discussion of the results. Detailed results are tabulated in Appendix D.

Heat Rejection

Heat rejection from the radiator surface was calculated two ways. The first method studied the PGW as it entered and exited the radiator. Temperature probes at the inlet and outlet, combined with a flow meter, allowed heat rejection to be calculated using Equation 1:

$$Q = \dot{m} \cdot c_p \cdot \left(T_{inlet} - T_{outlet}\right) \quad (1)$$

where Q = heat rejection [watts]
$\dot{m}$ = PGW mass flow rate [kg/sec]
c_p = specific heat of PGW [kJ/(kg·K)]
T_{inlet} = radiator inlet temperature [K]
T_{outlet} = radiator outlet temperature [K]

Equation 1 actually calculated the amount of heat lost by the PGW. Theoretically, this may not equal the amount of heat rejected by the radiator; some of the heat lost by the PGW could have, for example, been transferred to the radiator and then conducted into the table. However, steps were taken in the design of the test article to decrease the magnitude of other heat transfer mechanisms. Thus, Equation 1 was expected to yield a good approximation of the radiation heat rejection.

The second method involved comparing the temperature distribution of the radiator with the environment temperature. Radiation heat rejection could then be calculated using Equation 2:

$$Q = F \cdot A \cdot \varepsilon \cdot \sigma \cdot \left(T_{radiator}^4 - T_{environment}^4\right) \quad (2)$$

where Q = heat rejection [watts]
F = view factor (1, in this case) [unitless]
A = radiator surface area [m^2]
ε = radiator emissivity [unitless]

σ = Stefan-Boltzmann constant (5.67×10^{-8}) [$W/(m^2 \cdot K^4)$]
$T_{radiator}$ = radiator surface temperature [K]
$T_{environment}$ = environment temperature [K]

Heat rejection was not calculated for each separate thermocouple reading; $T_{radiator}$ was calculated by averaging the radiator surface temperatures together, and $T_{environment}$ was calculated by averaging the 4 coupon temperatures together. Analysis showed this to be a reasonable approximation. A fourth-order averaging technique was used in both cases, where

$$T_{avg} = \sqrt[4]{\frac{\sum_{x=1}^{n} T_x^4}{n}} \qquad (3)$$

where n = number of temperatures to be averaged.

At steady state, assuming all other heat transfer from the radiator is negligible, the heat rejection as calculated by Equation 1 should equal the heat rejection as calculated by Equation 2.

Analytical results from Reference 8 were recomputed based upon the as-tested conditions listed in Appendix C, and the analytical results were compared with those that were obtained from Equations 1 and 2. See Figure 22 for the comparison for each test point.

Several things become apparent from this graph. First, Equations 1 and 2 yield slightly different results, but they trend together and the differences in the results are not unexpected given the nature of this test, ranging from 5 to 16%. Both equations also yield results comparable with the

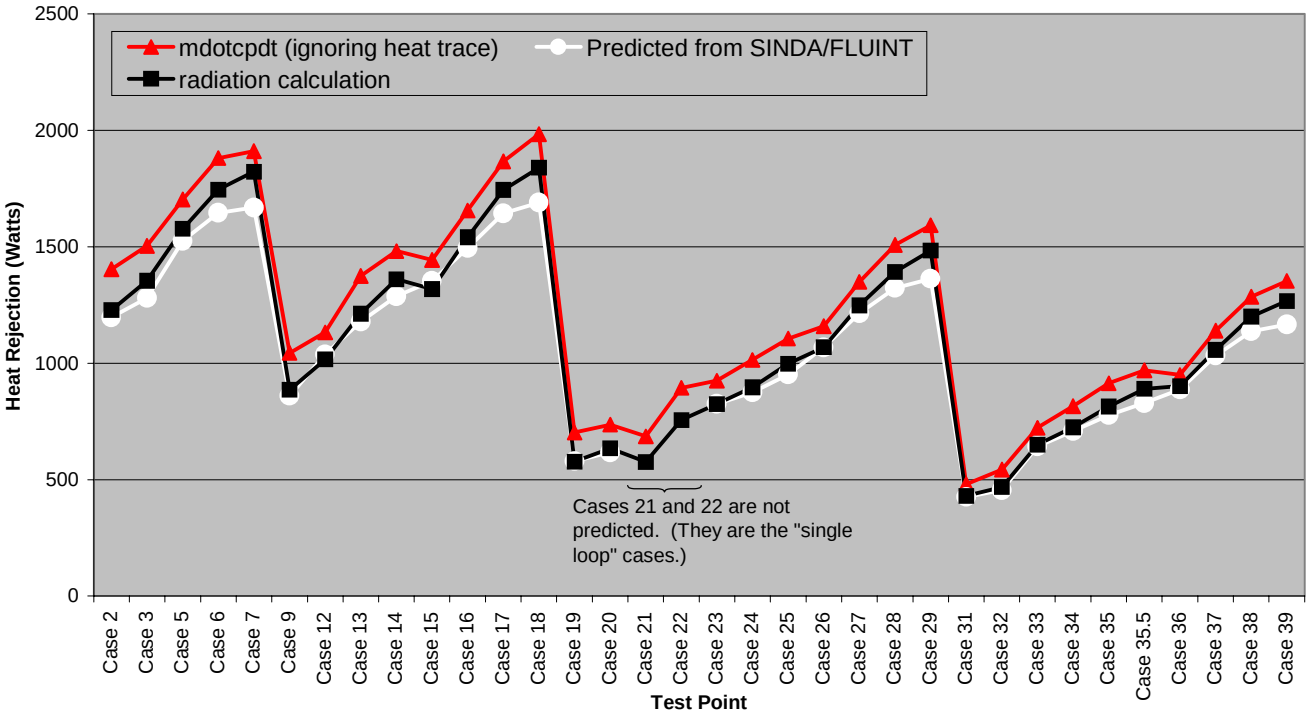

Figure 22 - FMF Radiator Test and Analysis Heat Rejection

analytical results.

When compared with the test point descriptions in Appendix C, the general behavior of the radiator is seen to be what would be expected: heat rejection increases with decreasing environment temperature, increases with increasing PGW inlet temperature, and decreases with decreasing PGW flow rate.

There are several things to note about these results. First, the analytical results were obtained assuming the radiator surface to be flat. In fact, the flow tubes rested on top of the radiating surface. Thus, the radiating surface area was not smooth, and it was larger than what was assumed, because of the presence of the tubes. The presence of the tubes was taken into account when estimating the area used in Equation 2. Thus, the analytical results under-predict the amount of heat rejection, perhaps by as much as 10%, and are not directly-comparable to those from Equation 2.

Also, there was some confusion caused by the heat traces on the lines running to and from the radiator. The heat traces were activated after Test Point 28 was performed, and they remained on for the remainder of the test. These heat traces were designed to warm the PGW upstream and downstream of the radiator. This would have had an effect on the results of Equation 1, because the radiator inlet temperature probes were not located at the radiator, but were instead approximately 3.75 meters (148") upstream of the radiator. These temperature probes were used to estimate T_{inlet} in Equation 1. Any heat imparted by the heat traces would have increased the inlet temperature above that registered at the temperature probe; thus, the value used for T_{inlet} would have been less than that actually at the radiator inlet. This would suggest that Equation 1 should have underestimated the amount of heat rejection for the cases following Test Point 28.

The tubing and heat traces were surrounded by insulation that should have forced most of the heat trace energy into the PGW. However, following an exhaustive study of the test data, no evidence could be found that the heat trace energy entered the PGW. To the contrary, interpretation of the data suggested that the energy did not enter the PGW. Ultimately, whether the heat trace energy entered the PGW could not be proved either way. However, based upon the engineering judgement of the Thermal Analyst assigned to this task, the presence of the heat traces was disregarded for all test points, and it was assumed, in concurrence with a preponderance of the evidence, that the heat traces did not have the intended effect on the PGW. If the heat trace energy did, in fact, enter the PGW upstream of the radiator, then Equation 1 underestimates the heat rejection by an amount equal to the heat trace energy that was disregarded; this amount ranged from approximately 60 to 80 watts, depending upon the test point.

Some of the difference between the results of Equation 1, Equation 2, and the analytical results can be explained by the accuracy of the instrumentation used in this test. An uncertainty analysis indicated that the results of Equation 1 have an uncertainty of about ±15 watts, and the results of Equation 2 have an uncertainty of about ±20 watts. The amount of uncertainty varies and is dependent upon the actual Test Point. A more detailed listing of the heat rejection results, including the amount of uncertainty for each test point, is included in Appendix D.

One area in which the analytical model could be improved is for low flow rate cases. The test article showed a more significant drop in the heat rejection between the 100 and 50 lb/hr cases than was predicted by the model.

One aspect of the radiator that influences heat rejection is its ability to spread heat uniformly throughout its surface. If it were designed with a low thermal conductivity, then areas between the flow tubes would remain cool, decreasing heat rejection. The surface between each tube may be regarded as a fin, and a "fin efficiency" can be determined to quantify how readily heat transfers from the flow tubes to, and throughout, the woven aluminum. As stated in the Instrumentation section above, TCs were placed on the radiator to determine the temperature distribution between flow tubes. The results for 7 Test Points are shown in Figure 23.

Refer to Figure 19 for an explanation of the placement of the thermocouples. In summary, the fin efficiency was evaluated at 4 locations with four groups of TCs (31-37, 38-44, 45-51, and 52-58). Figure 23 indicates that the woven aluminum spread heat from the flow tubes well. If it had not, the lines in Figure 23 would have been "dome-shaped", with a high temperature at the thermocouples nearest the flow tube, and lower temperatures on either side. Instead, the temperatures are uniform around each set of flow tubes. Similar plots were prepared for the other test points. Similar temperature profiles were seen for all test points except the "single-loop" test points of 21 and 22, which tended to show a slight, inverted "dome" around the

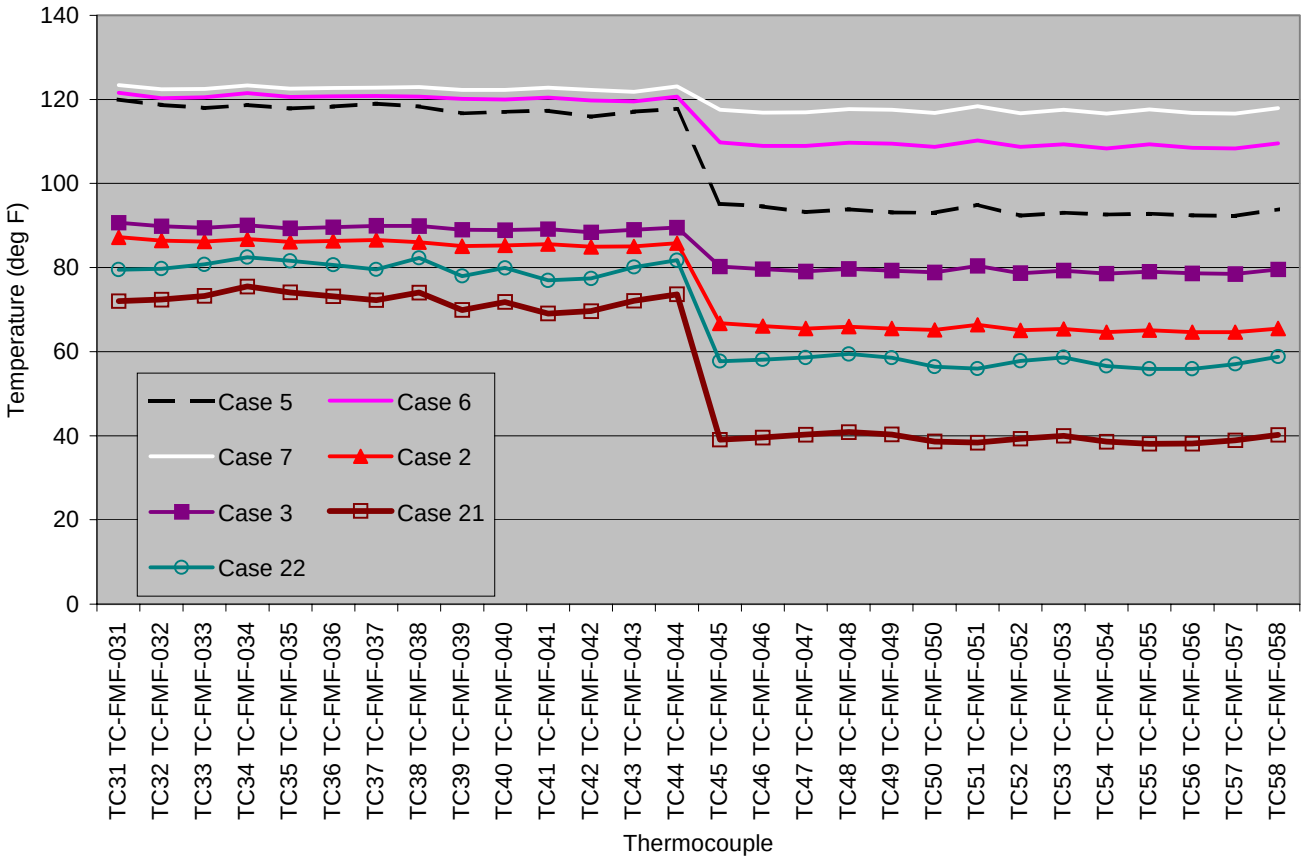

Figure 23 - FMF Radiator Fin Efficiency

"failed" loop, which was as expected, since the failed loop was not transferring heat to the radiator.

Pressure Drop

Figure 24 shows the pressure drop seen through each loop in the radiator for each test point. As can be seen, pressure drop decreased with decreasing flow rate, but a large spread existed in the results at any given flow rate. The reason is that temperature affects the viscosity of PGW; thus pressure drop through the system is also a function of the radiator inlet temperature. A trial-and-error approach revealed that, for this test, pressure drop was approximately related to temperature and flow rate through Equation 4:

$$\Delta p \approx \frac{F}{T - 30} \qquad (4)$$

where Δp = pressure drop through the radiator [psi]
F = flow rate per loop [lb/hr]
T = inlet temperature [°F]

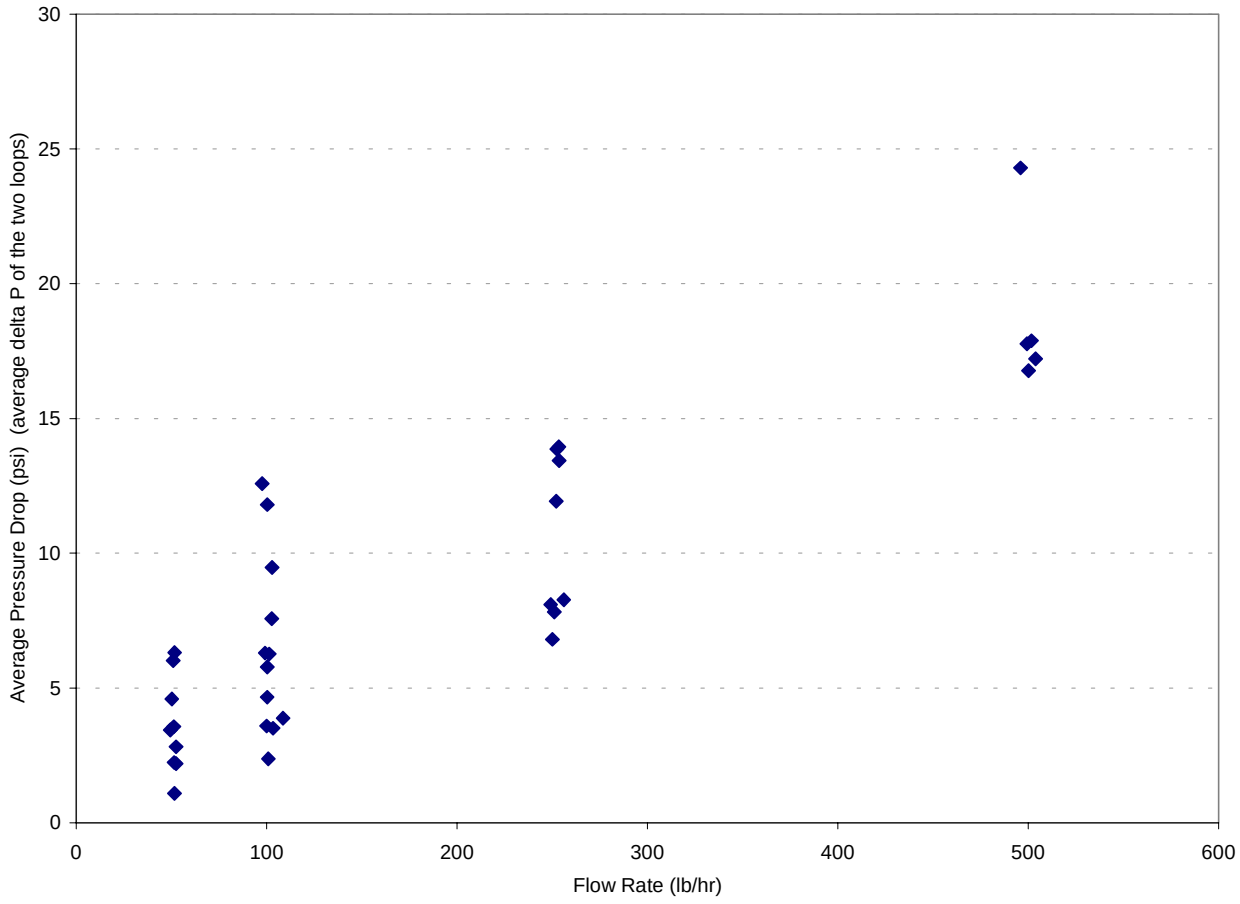

Figure 24 - FMF Radiator Pressure Drop

The maximum pressure drop in the system was 24.3 psi for Test Point 35.5 (45°F environment, 100°F inlet temperature, 500 lb/hr flow rate).

Flexibility

A test was performed to gauge the flexibility of the FMF radiator after the thermal/vacuum test, according to Reference 15. During the flexibility test, the FMF radiator was manually placed against rounded objects of varying radii. It successfully conformed to the shape of the rounded objects with radii of 5.5", 3.375", and 2.5". However, it would not conform to an object with a radius of 1.125". This confirmed the flexibility of the radiator for radii of curvature equal to or greater than 2.5". Note that the radiator was bent only around an axis parallel to the flow tubes; since the flow tubes are not flexible (only the woven material to which they were attached was designed to flex), the radiator would have been damaged had any attempt been made to bend the radiator around an axis perpendicular to the flow tubes.

Comparison with Advertised Performance

The FMF radiator was designed and built to TransHab requirements and should have performed as follows:

1. 594 W of heat rejection in an environment of 241K @ 500 lb/hr flow rate, 65°F inlet temperature
2. 849 W of heat rejection in an environment of 155 K @ 500 lb/hr flow rate, 65°F inlet temperature
3. maximum pressure drop of 30 psid @ 500 lb/hr
4. 3" bend radius

The radiator was not tested at these conditions, but analysis of the existing data confirmed that the radiator would have met these capabilities had it been tested at these conditions.

Specifically, Test Point 20, which had an inlet temperature of 64°F, was tested at a warmer environment, and a lower flow rate, than listed in Requirement 1 above. However, it rejected 735 W or 635 W (depending upon whether Equation 1 or Equation 2 is used). Had the radiator been tested at the colder environment of 241K, with a higher flow rate of 500 lb/hr, it is reasonable to assume that it would have rejected in excess of 594 W.

Similarly, note Test Point 9, which had an inlet temperature of 64°F, and which was tested at an environment of 228K with a flow rate of 98 lb/hr. Heat rejection during Test Point 9 was either 1044 W or 886 W, depending upon whether Equation 1 or Equation 2 is used. Had the radiator been tested at the colder temperature and higher flow rate of Requirement 2 above, it surely would have exceeded the 849 W required.

A disclaimer must be made: the radiator showed a tendency to freeze at colder environments for the low flow rate cases. Successfully meeting the first and second Requirements listed above is contingent upon the radiator not freezing at the actual conditions. Whether it would have frozen

at the required conditions is unclear; the colder environments would have significantly increased the likelihood of freezing, but the higher flow rate, 500 lb/hr, would have diminished the likelihood of freezing.

The pressure requirement was met, as the pressure drop did not exceed 30 psi during any test points.

Finally, the flexibility requirement was met, as it was able to bend around an object whose radius of curvature was less than 3".

Loop Heat Pipe and Carbon Fiber Fin Radiator Results

As stated earlier, and as can be seen in Appendix C, most of the LHP test points were successfully completed, albeit with modifications to the environment temperature requirements. Heat rejection was evaluated at these test points. Additionally, pressure drop was determined at different operating flow rates, and the flexibility of the radiator was confirmed. Prior to the test, the mass per radiating area of the LHP radiator was found to be 6.4 kg/m^2 (not including the mass of any coolant in the system).

Much of the analysis for the LHP radiator mirrored that of the FMF radiator. This section does not repeat the overview and discussion provided in the previous section on such topics as the heat trace and fin efficiency; the reader is encouraged to review the FMF radiator results section for additional information on these topics. This section gives an overview and discussion of the LHP radiator results. Detailed results are tabulated in Appendix E.

Heat Rejection

As for the FMF radiator, heat rejection by the LHP radiator was calculated using Equations 1 and 2 above. Average temperatures were calculated using Equation 3. However, unlike with the FMF radiator, the LHP radiator results from Equations 1 and 2 should not be equal; the heat rejection from the radiator, as calculated by the radiation equation (Equation 2) should equal the sum of the heat supplied to the system (Equation 1) plus the heat supplied to the system by the Variac heaters (used on the "dummy" loop heat pipes). An energy balance on the system is listed below as Equations 5 and 6:

(Energy Rejected by the LHP Radiator) = (Energy Supplied to the LHP Radiator) (5)

or

(Q from Equation 2) = (Q from Equation 1) + (Heat Supplied by the "Dummy Heaters") (6)

As for the FMF radiator, the energy balance assumes that there are no other heat transfer mechanisms present (such as conduction to the radiator support table). Steady state conditions are also assumed.

The results from this energy balance are plotted in Figure 25 for each LHP test point. Note that the line with square markers (which is simply the sum of the lines without markers) was expected to equal the line with diamond markers.

Several things are apparent from Figure 25. First, there is excellent consistency in the two methods of calculating heat rejection for Test Points 19 and beyond. This shows confidence in using both methods of calculating heat rejection for this system. However, the earlier test points do not show an agreement between these two methods. Despite considerable analysis of the available data, this phenomenon was never fully explained, but certain observations were made.

It was noted that the radiation calculations (Equation 2), shown by the line with diamond markers in Figure 25, showed a consistent trend throughout, whereas the results from Equation 1 were erratic and are inconsistent with the expected results. Thus, there is a higher degree of confidence in the results of Equation 2.

Analysis of the data revealed unusual behavior in the LHP PGW outlet temperature reading. Although it gave reasonable data for the warmer environment cases and for the low flow cases, it tended to register unrealistically high readings in the cold environment cases, especially as flow

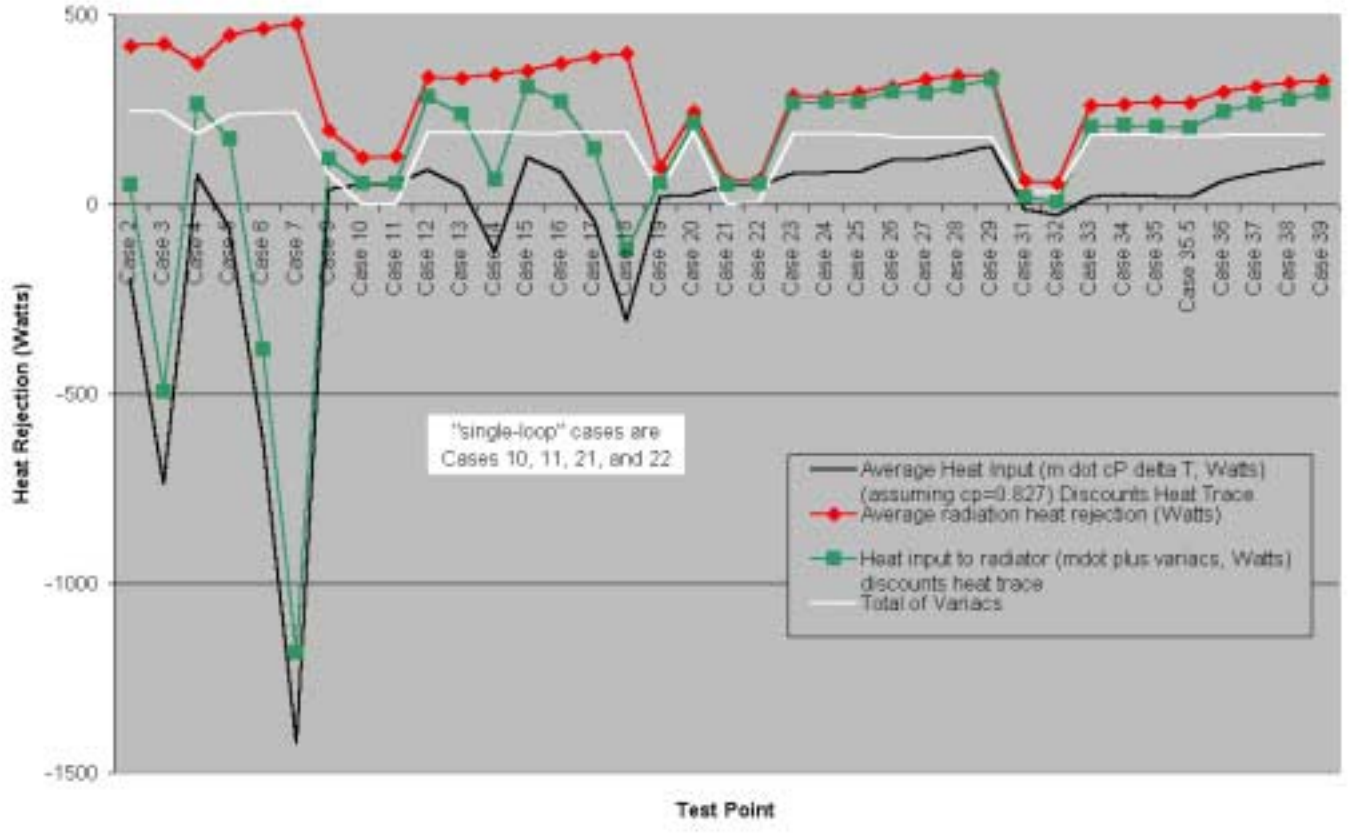

Figure 25 - LHP Radiator Test Heat Rejection

to the LHP radiator increased. The results of this can be seen clearly in Figure 25 for Test Points 15 through 18.

Test Points 15 through 18 all were at the same environment temperature and inlet temperature. Flow rate increased from 50 to 500 lb/hr from Test Points 15 through 18, respectively. As the flow rate increased, the LHP PGW inlet temperature probe confirmed constant inlet temperatures, but the outlet temperature probe began recording increasingly high temperatures, beyond expectations. This accounts for the apparent decrease in heat rejection by the radiator. It also accounts for the apparent heat absorption (negative heat rejection) by the radiator for some cases. Analysis of the data suggests that the radiator was never absorbing heat, but that the PGW outlet temperature probe gave erroneous data at the low environment temperatures, and increasingly erroneous data for increasing flow rates. Cavitation at the probe was offered as a reasonable explanation for this phenomenon.

As such, the radiation heat transfer (as calculated by Equation 2) is considered the more accurate set of data for this test.

It should be noted that the effects of the heat trace were disregarded for the LHP radiator analysis, as was done for the FMF radiator analysis. Also of note is the emissivity of the radiator: As discussed previously, flaking of the Z-93 caused significant parts of the Mylar® to be exposed. This would have decreased heat rejection, as the exposed Mylar® has a lower emissivity than that of Z-93. The effects of the flaking were disregarded in this analysis, and an overall emissivity of 0.90 was assumed. Thus, the results predicted by Equation 2 are slightly high. Introducing a lower emissivity to account for the flaking would have the effect of bringing the results of Equation 2 more in-line with those of Equation 1.

Based on the results of Equation 2, the LHP behaved generally as expected: heat rejection increased with decreasing environment temperature, heat rejection increased with increasing inlet temperature, and heat rejection increased with increasing flow rate.

As was done for the FMF radiator, the "fin efficiency" of the LHP radiator was evaluated. Figure 26 plots the results for 12 Test Points. Refer to Figure 20 for a description of the thermocouple numbers.

Unlike for the FMF radiator in Figure 23, a "dome" shape is readily apparent in Figure 26, indicating that heat was accumulating in the vicinity of the loop heat pipes. This suggests that one area of improvement could be in improving heat transfer throughout the radiator surface. Results were similar for the test points not shown in Figure 26, however a tendency for the dome to "flatten out" was observed for test points having a lower inlet temperature. This was not unexpected; higher loop heat pipe temperature would be expected to yield a "spike" in radiator temperatures at the loop heat pipe if lateral conduction through the radiator were low.

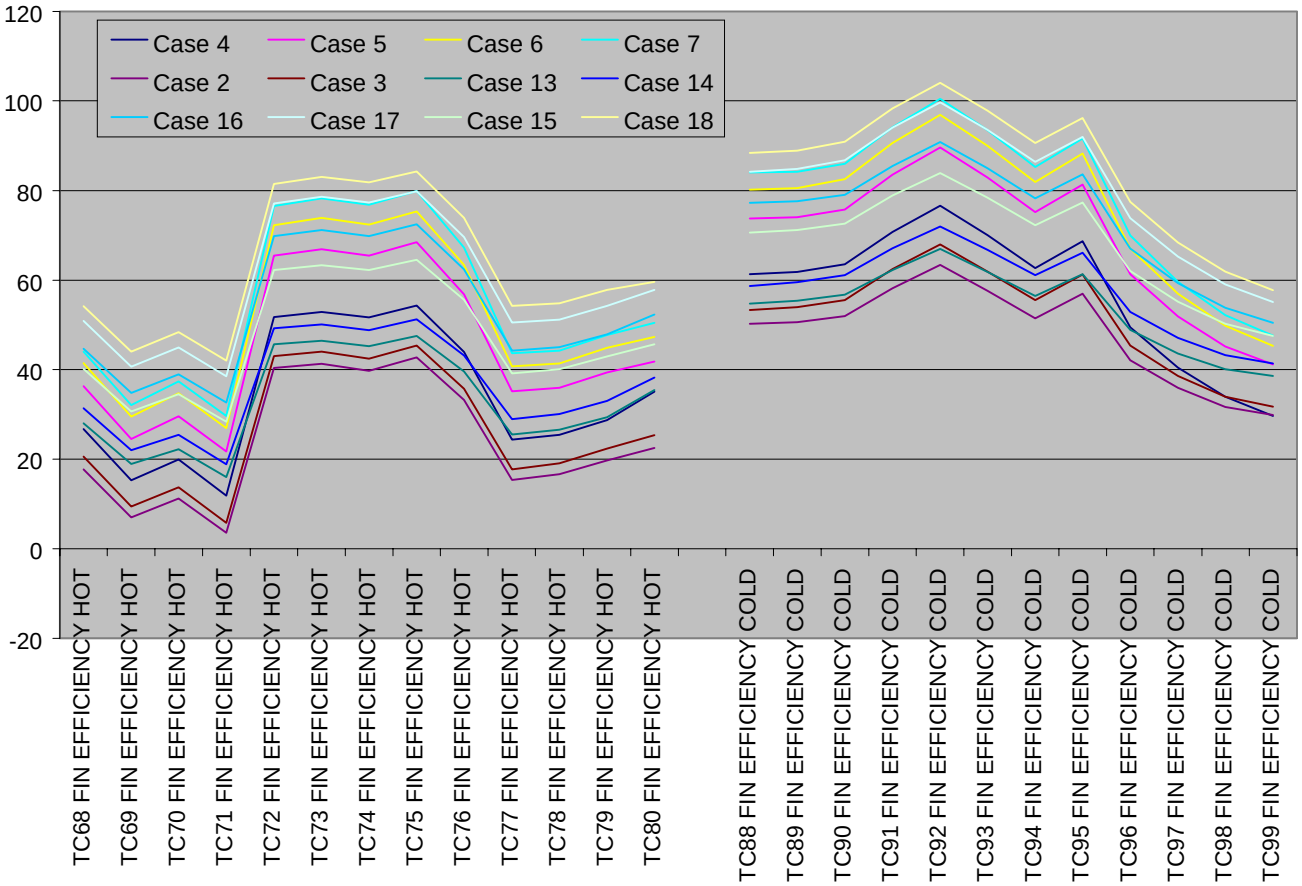

Figure 26 - LHP Radiator Fin Efficiency

Pressure Drop

Figure 27 shows the pressure drop through the LHP radiator for each test point. The pattern is similar as that seen for the FMF radiator, for the same reasons: pressure drop is a function of both PGW flow rate and inlet temperature. As was done for the FMF radiator, a trial-and-error approach was used to develop an equation which roughly predicted the pressure drop as a function of inlet temperature and flow rate. This is shown below as Equation 7:

$$\Delta p \approx \frac{(F + 20)^{1.8}}{T - 30} \qquad (7)$$

where Δp = pressure drop through the radiator [psi]
F = flow rate per loop [lb/hr]
T = inlet temperature [°F]

The maximum pressure drop in the system was 3.54 psi for Test Point 35.5 (45°F environment, 100°F inlet temperature, 500 lb/hr flow rate). This is the same test point that yielded the highest pressure drop for the FMF radiator. The pressure drop for the LHP radiator was much smaller

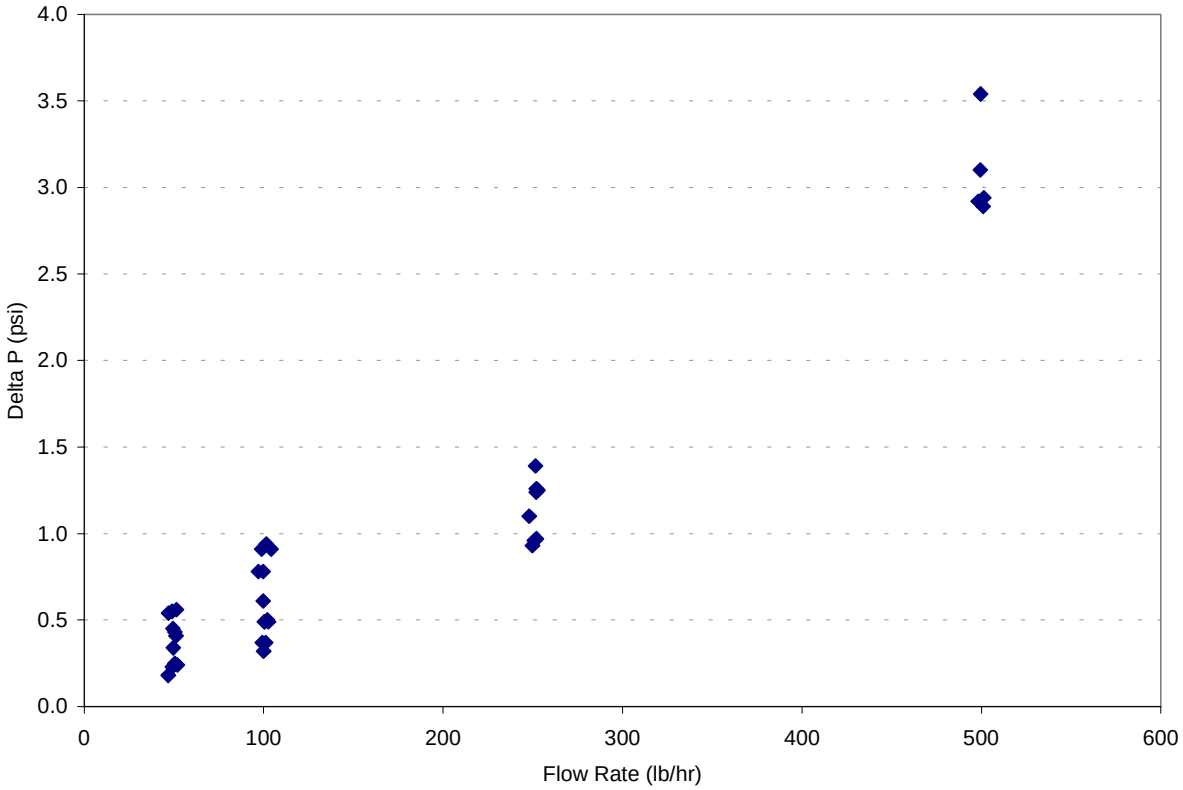

Figure 27 - LHP Radiator Pressure Drop

than for the FMF radiator because the flow was not required to pass through numerous small-diameter tubes.

Flexibility

The flexibility of the LHP radiator was tested before the thermal/vacuum test. Manual handling of the radiator determined that the radiator could "fold" along an axis parallel to the loop heat pipes. This could only be done between each loop heat pipe, as the loop heat pipes themselves were not flexible. The radius of curvature was not measured when it was folded, however, observation confirmed that it was negligibly small.

Comparison with Advertised Performance

The LHP radiator was designed and built to Transhab requirements and should have performed as follows:

1. 191 W of heat rejection in an environment of 241K @ 1000 lb/hr flow rate, 65°F inlet temperature
2. 276 W of heat rejection in an environment of 155 K @ 1000 lb/hr flow rate, 65°F inlet temperature
3. maximum pressure drop of 1.4 psid @ 1000 lb/hr

4. 3" bend radius

The radiator was not tested at these conditions, but analysis of the existing data confirmed that the radiator would have met the first requirement had it been tested at that condition.

Specifically, Test Point 20, which had an inlet temperature of 64°F, was tested at a warmer environment, and a lower flow rate, than listed in Requirement 1 above. However, it rejected 244 W (based upon Equation 2). Had the radiator been tested at the colder environment of 241K, with a higher flow rate of 1000 lb/hr, it is reasonable to assume that it would have rejected in excess of 191 W.

Data could not confirm whether the second requirement could be met; the radiator was not tested at an environment of 155 K, and it rejected less than 276 W for more moderate conditions. Extrapolation of the data to consider an environment of 155 K was not possible with any degree of accuracy.

The third requirement, relating to pressure drop, was not met. The radiator exhibited pressure drops well in excess of 1.4 psid for flow rates lower than 1000 lb/hr.

The flexibility requirement was met.

Carbon Velvet Cold Plate Results

The thermal performance of the Carbon Velvet Cold Plate was successfully evaluated in vacuum conditions. Results are shown in Table 11 of Appendix F.

First, the temperature distributions throughout the cold plate were examined. Figures 28 through 31 show the temperatures from the surface-mounted thermocouples mounted on each component of the cold plate assembly.

These temperatures are representative of the other test cases. The numbers on each graph are the thermocouple numbers. Generally, the temperatures were uniform. This indicates that the heaters worked well.

PGW enters the cold plate on the right side of each graph and flows to the left. The effects of this can be seen in Figure 31, with the temperature increasing from the right to the left as the coolant acquired heat flowing through the cold plate. The other graphs indicate that the temperatures on the "lower" side of the cold plate (as shown in the graphs near TC-CP-11 and 20) were slightly warmer. Other test points show more dramatic hot spots in this location. These warm spots appear to be exaggerated due to errors with TC-CP-11, as explained previously in this report.

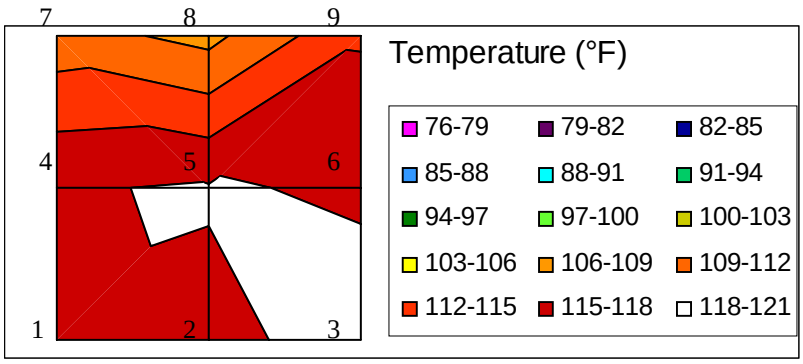

Figure 28 - Heated Surface of Top Set of Radiant Fins, Test Point 40

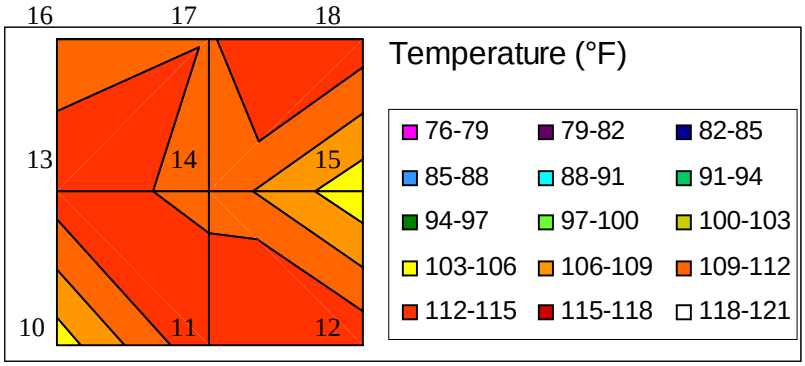

Figure 29 - Base of Fins, Top Set of Radiant Fins, Test Point 40

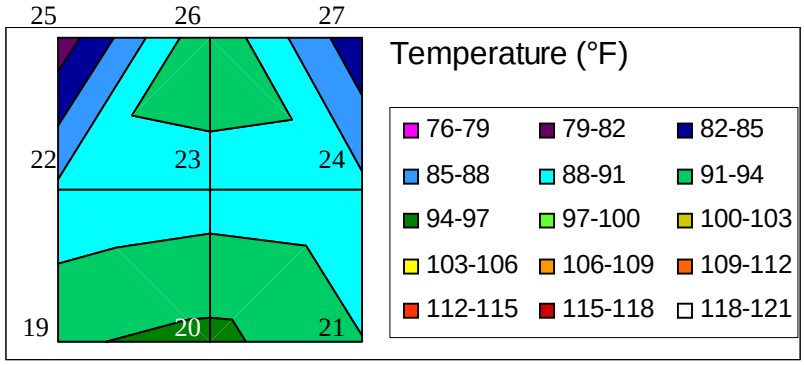

Figure 30 - Base of Fins, Bottom Set of Radiant Fins, Test Point 40

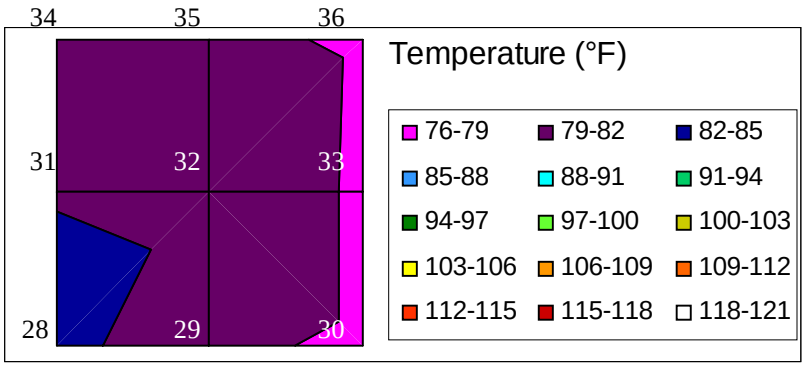

Figure 31 - Cold Plate, Test Point 40

Next, a comparison between the heat removed by the coolant and the electrical power input to the heaters was made. Heat removed by the coolant was calculated using the absolute value of Equation 1, and the power input to the heaters was measured directly from the data acquisition system. Uncertainties for this heat removed were, on average, ±4.5 W for the 125 lbm/hr flow rate test points and ±37 W for the 1100 lbm/hr test points. Uncertainties for each test point are found in Table 11 of Appendix F. Figure 32 shows that these values agreed well for Test Points 40, 41, and 47 through 55. However, Test Points 42 through 46 show that much more heat is being removed from the cold plate via the coolant than is added by the heaters.

Upon a more detailed review of the data, it was determined that Test Points 42 through 46 had not reached steady state even though the steady state criteria outlined in the DTP (and in the Test Summary section of this document) had been met. The first indication was that the energy entering and leaving the cold plate were not equal, as seen in Figure 32. In addition, the test points with the greatest difference between these values were performed after there was a large change in the heater power applied to the test article and a large change in the coolant flow rate provided to the cold plate. Test Point 43 had the largest discrepancy. This could be explained by a short period before the test point where the heater power had been turned up to 2000 W, twice as much as the 1000 W for the test point, providing another large step change in the heat load applied to the test article.

Figure 33 was created to examine Test Point 43 in more detail. It adds to the argument that the test point had not actually reached steady state. This figure shows the heat removed by the coolant and the power applied to the heaters for Test Point 43 as a function of time. It shows that the power applied to the cold plate through the heaters was constant and that the heat removed by the coolant was decreasing from a higher value, which corresponded to the period of time the heaters were set to 2000 W. This heat removed curve is a characteristic asymptotic transient curve. It appears from the graph to have leveled out by the 30 minute period that was used for

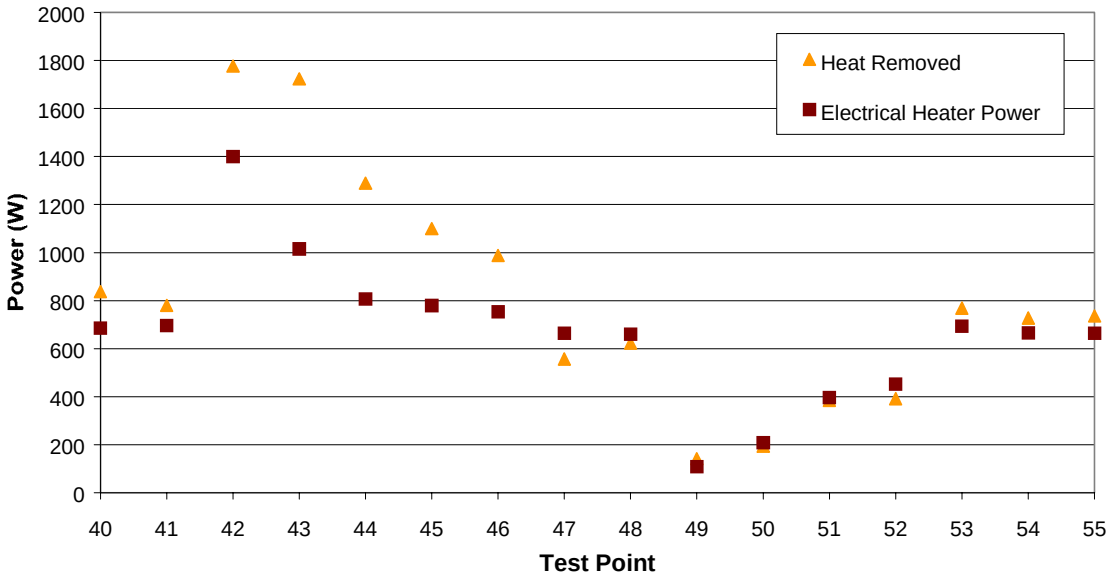

Figure 32 - Cold Plate Energy Balance

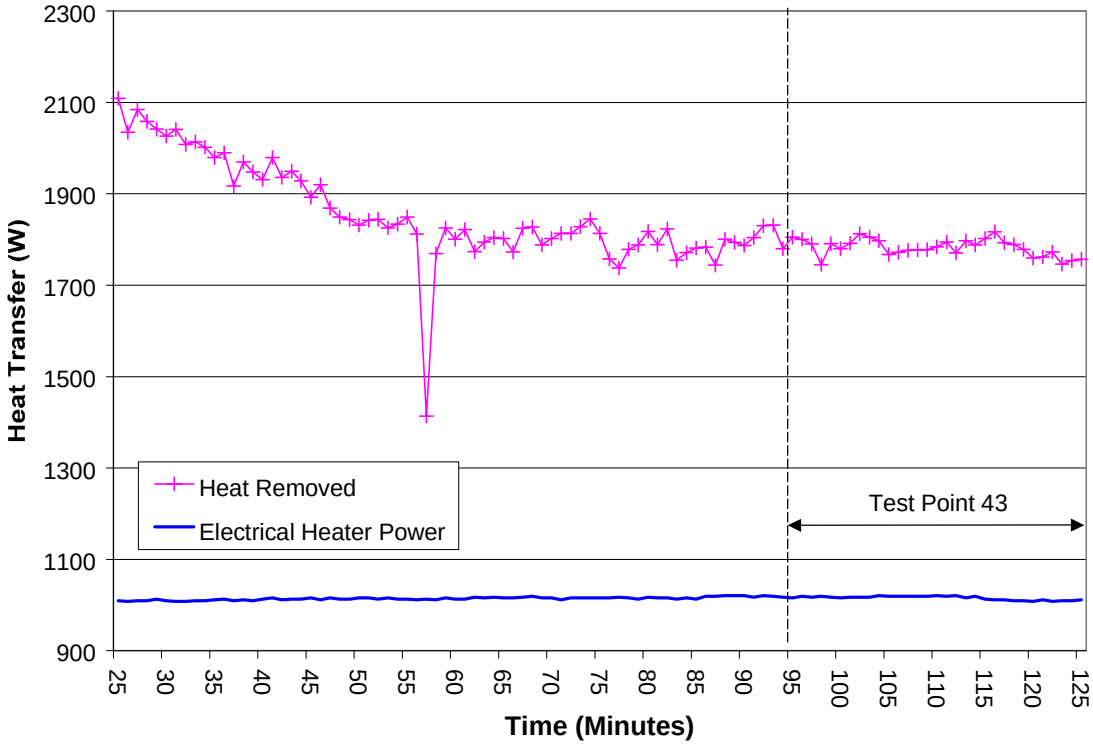

Figure 33 - Cold Plate Heat Removed and Electrical Heater Power, Test Point 43

the test data. This would indicate that the cold plate test article had reached steady state. However, it was determined post-test that the slope of this line is about 100 W/hr. This is very significant for a 1000 W test point.

It was also found that some test points showed changes in temperature on the order of 0.5 °F during the 30 minute "steady state" period that made up each test point. Upon review of the test data, it was discovered that a change in temperature of this magnitude, although seemingly small, has a large effect on the heat rejection as calculated by Equation 1. This was a result of the relatively large flow rate used in this test.

All of these factors indicate that, even though the Carbon Velvet Cold Plate had met the DTP steady state requirements, many of the test points do not actually represent steady state conditions.

Another key parameter used to evaluate the performance of the cold plate was the average surface temperature of the heated surface as a function of heat load. Figure 34 shows this relationship using the electrical power to the heaters as the heat load.

Figure 34 shows that the surface temperature of the cold plate increases linearly with increasing heat load. This trend was expected because the primary heat transfer mechanism through the cold plate was conduction, which has a linear relationship between heat transfer and temperature. Figure 34 also shows a discontinuity in the slope of this trend at a heat load of around 750 W.

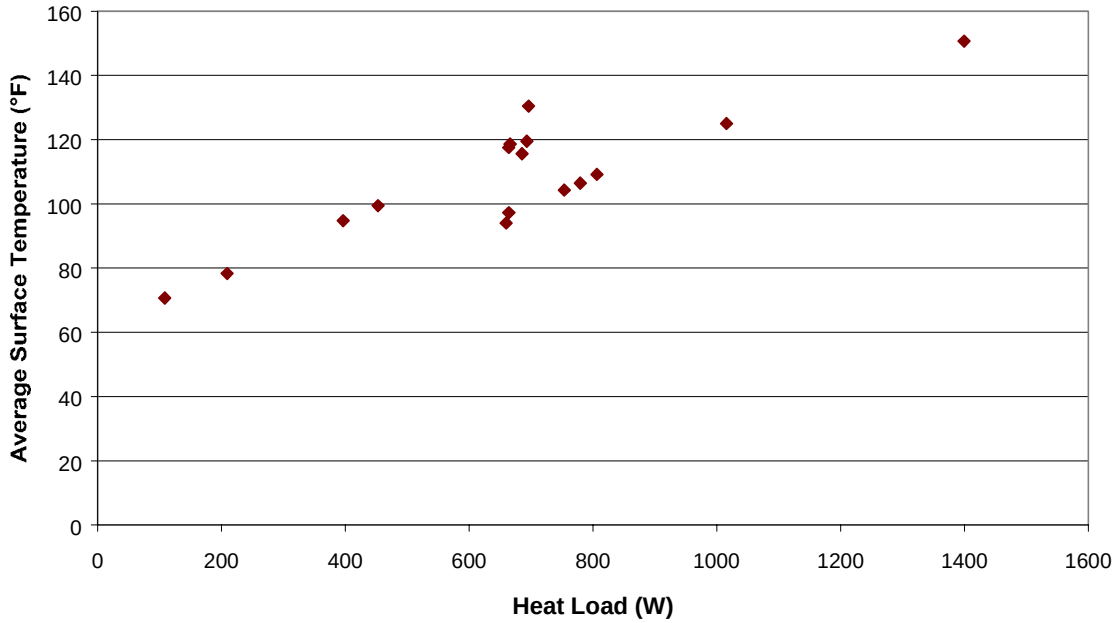

Figure 34 - Cold Plate Average Surface Temperature vs. Heat Load

All of the data with heat loads greater than this value correspond to the test points that had not yet reached steady state.

Average surface temperature is a critical parameter in evaluating a cold plate because it indicates the temperature of the hardware the cold plate was designed to cool. The test team had set a goal of 100°F for surface temperatures of the cold plate. The Space Station Freedom temperature limit for a DC – DC Converter (the avionics that this cold plate was intended to cool) was 130°F [16]. The target heat load was 694 W, from the ISS cold plate specification [14].

Disregarding the test points that had not reached steady state, the data show that the Carbon Velvet Cold Plate could handle a 664 W heat load while maintaining the heating surface temperature below 100°F, and 696 W with a corresponding surface temperature of 130°F. Test Point 40, which was run at the actual ISS conditions of 125 lbm/hr flow rate, 39°F inlet temperature, and 694 W heat load, resulted in a surface temperature of 115°F. This means that the Carbon Velvet Cold Plate met the ISS requirements and almost met the test team's desired performance.

The final parameter used to quantify the Carbon Velvet Cold Plate performance was the temperature drop across the carbon velvet-radiant fin interface. Figure 35 shows the temperature difference between the average temperatures at the base of the fins on each radiant fin set as a function of the electrical power to the heaters.

This trend is also linear, as expected for heat transfer by conduction. It should be noted again that all test points with a heat load over 750 W were from test points that had not reached steady state.

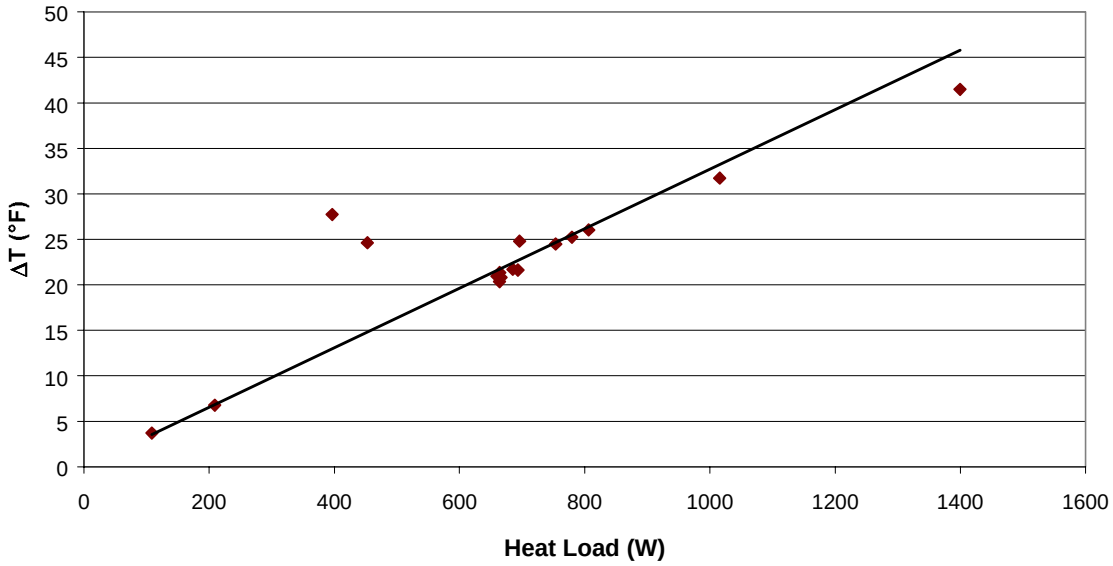

Figure 35 - Temperature Drop Across Carbon Velvet Fin Interface

A line fit through these data gives a heat transfer resistance (R) of 0.0327°F/W, which corresponds to the slope of the line. This resistance corresponds to a heat transfer coefficient (h) of 189 W/m²·K (h = 1/RA, where A is the cross-sectional area of the conduction path for the cold plate, 21 in x 21.5 in = 451.5 in²). These results were compared with experimental results from the manufacturer, listed in Table 2.

Table 2 - Cold Plate Performance Summary

Performance	Radiant Fin Interface [17]	Carbon Velvet Fin Interface [17]	Carbon Velvet Cold Plate
h (W/m²·K)	~ 70	170 – 540	189
ΔT (°F)	~ 36	5 – 15	13 – 28

Ranges are reported from the ESLI testing because several different carbon velvet configurations were tested [17]. The Carbon Velvet Cold Plate heat transfer coefficient across the fins, 189 W/m²·K, was determined to be within the range predicted by ESLI.

The temperature difference across the fins (ΔT) corresponds to a heat flux of 1400 W/m^2, or 406 W for our test article. A range is reported for the Carbon Velvet Cold Plate Chamber B test data because there is a large difference between the actual measured values and the value predicted by the trend in Figure 35. The two test points in Figure 35 that compare with a 406 W heat load had temperature differences of 28 and 25°F, for heat loads of 397 and 453 W, respectively. (This is the source of the high end of the 13 - 28°F range reported.) However, these two points correspond to Test Points 51 and 52 and do not follow the trend of the other data. A detailed look at these test points indicated an extremely high reading on TC-011, as discussed previously, that skewed the average fin base temperature used in calculating the temperature difference. Since these temperature differences seem to be skewed by this high temperature anomaly, the temperature difference across the fins was predicted using the trend in

Figure 35. This predicted a difference of 13°F, at a 406 W heat load, which corresponds to the high end of the data reported by ESLI.

CONCLUSIONS/FINDINGS

These test articles did not always function as expected, but the test was a success: the test objectives were met, and valuable data were collected on the performance of the test articles.

Performance data for a wide variety of environment temperatures in a vacuum were collected for the FMF radiator; and it was tested across a wide range of inlet temperatures and flow rates. The radiator was not tested at the design criteria. However, assuming it would not have frozen, the FMF radiator would have met the design heat rejection requirements while maintaining a pressure drop below the maximum allowable levels. It also met the flexibility criterion.

Also, performance data for a wide variety of environment temperatures in a vacuum were collected for the LHP radiator; and it was tested across a wide range of inlet temperatures and flow rates. The radiator was not tested at the design criteria. However, the LHP radiator would have met at least some of the design heat rejection requirements. A complete evaluation of its performance was not possible because the chamber did not provide a sufficiently cold environment. It failed to meet the pressure drop requirements, but it met the flexibility criterion.

The Carbon Velvet Cold Plate performed better, with respect to the heat transfer coefficient through the fins and the temperature drop across the fins, than a traditional radiant-fin cold plate, and as well as advertised by ESLI. The Carbon Velvet Cold Plate met the ISS requirements for heat load and surface temperature. However, it did not meet the test team's goal of maintaining a surface temperature of less than 100°F for the desired heat loads.

LESSONS LEARNED

During the course of planning for this test, build-up, and post-test analysis, numerous lessons were learned that may help during the performance of future tests. These "lessons learned" are discussed below.

- A binder was prepared before the test summarizing the instrument placement, listing the test points, and describing the test articles. This was found to be extremely helpful during the test, and helped the TRs conduct an efficient and fairly trouble-free test. The importance of training the TRs before the test, so that they are equipped to handle off-nominal conditions, can not be overemphasized.
- TRs were required to keep a log book during the test. Useful things that were noted in the log book included not only the actions that were performed during the test, but also the rationale behind it. The log book proved to be a valuable record, especially post-test when it was necessary to reconstruct events to explain sometimes-confusing data. Maintaining a clear and complete log book during the test, in which the TR documents his or her thought processes, was vital to the post-test analysis efforts. Prior to future tests, all TRs should receive training on how to clearly and completely document their actions. This training should emphasize the need to document the rationale behind any

action taken.

- Engineers should consider before the test how small fluctuations in certain data points might propagate through the calculations to yield huge errors or fluctuations in calculated parameters. For this test, a small change in the cold plate outlet temperature translated into a huge change in heat rejection because of the high flow rate. As stated earlier in the report, this made satisfying the test objectives more difficult, because the TR was not always able to determine from the instrumentation when steady state had been achieved. In future tests, ways should be investigated to minimize this likelihood while still meeting the test objectives.
- To simplify the post-test analysis, the TR should be very specific in how he or she wants the data formatted when received after the test. EC4 has the ability to format data in a variety of ways, some of which are easier to work with than others. Data received in fewer but larger files were easier to work with than data received in numerous, smaller files. The TR should request data be delivered in the most useful unit system.
- The TR should carefully plan ahead and determine the most efficient order for the test points. All of the "difficult" test points should be grouped together (preferably at the end of the test) so the plan does not become too confused if they must be abandoned. For this test, problems developed with low temperatures (freezing) and high flow rates (the cart could not always produce enough flow to get 500 lb/hr to both radiators simultaneously). These test points should have been attempted last. Also, order the test points to make the transition from one point to another as easy as possible. For example, instead of varying several parameters between test points, try to arrange the test points so only one is varied at a time.
- Consider making test articles as small as possible, not as large as you can afford. After verifying basic principles, larger products can be developed.
- One valuable tool during this test was an excellent photo-record of the test articles before and after the test. A video camera with an audio description might be preferable to still pictures.
- Although this test was well-performed with the personnel assigned to it, it should be emphasized that responsibilities for planning the test and for overseeing the build-up should be shared among people with different backgrounds. This will help ensure that critical issues are not overlooked. For example, the analyst may have the best insight into the proper placement of instrumentation, since he or she will be responsible for deciphering the corresponding test data, whereas the instrumentation engineer may have the best knowledge of which instruments are most suited for a particular task, and the test requester can also provide inputs to ensure that the instruments are sufficient to satisfy the test objectives. Any single person will not have a broad enough background to adequately prepare for any major test, since tests are comprised of many varied subject areas.
- It would have been useful if the resources had been available to conduct a repeatability test to verify the accuracy of the measurements. For example, would the same results have been obtained going from 50→100→250→500 lb/hr as would have been obtained going from 500→250→100→50 lb/hr flow rate?
- Numerous people were involved with developing the three test articles included in this test. Both the radiators and cold plate projects passed through many people, creating inconsistencies and unconsolidated information. Also, both radiators, and several others that were not tested, were developed to nearly the same, but different specifications.

Comparison of these radiators was complicated by these inconsistencies. The development of these pieces of hardware, and their specifications, would have been more consistent and better organized if the individuals working on the projects had stayed with the projects to the completion.

- Several of the cold plate test points were determined to not have reached steady state even thought the steady state criteria in the DTP had been met. When defining steady state criteria, the TR should consider the last part of the hardware to change temperature.
- Prior to the test, there was concern over using adhesive heaters. Previous experience had shown a tendency for air bubbles to become trapped under the heaters during application. Once in vacuum, those bubbles would expand and dislodge the heaters, preventing the heater from contacting the test article. This created a hot spot that would cause the heater to burn out or to damage the test article. However, the Minco® heaters with aluminum backing used in this test worked well and did not have any of these problems.
- The importance of functional testing of support equipment is essential to having a successful test. Functional testing was often shortened or skipped due to schedule constraints. An example was that the Filtrine carts were not able to provide 500 lbm/hr to multiple test articles, the Filtrine Cart #1 controller did not work, and Filtrine Cart #5 had electrical problems leading to a smoking terminal block. These problems were then resolved during the test, which consumed valuable test time. This also applies to Chamber B itself. Little maintenance or functional testing of the chamber led to having to fix facility problems during the test.
- Controlling the environments with the heater slats did not work as well as advertised. Environments were difficult to control and many of the desired environment temperatures were never reached. This was complicated by interaction between the radiator and the coupons.
- This test was expensive to run. The original plan called for the testing of 5 radiators, but the test was scaled-back to accommodate budget constraints. The knowledge of testing costs that was gained during this test will help with future planning.
- In an effort to reduce test cost, D. Westheimer/JSC/EC2, B. Macias/JSC/EC4, E. Chan/JSC/EC4, and M. Halligan/JSC/EC4 all participated in the physical build-up of the test. These activities provided valuable hands on experience as well as experience with documentation, writing procedures, and the quality system.

REFERENCES

1. "Advanced Radiator Concepts Thermal/Vacuum Test Test Requirements and Test Plan Document", Revision A, David Westheimer/JSC/EC2, CTSD-ADV-466, JSC-40060, March 15, 2001.
2. "Carbon Velvet Coldplate Thermal/Vacuum Test Test Requirements and Test Plan Document", Revision Basic, David Westheimer/JSC/EC2, CTSD-ADV-475, JSC-47625, April 5, 2001.
3. Filtrine Manufacturing Company, 15 Kit Street, Keene, NH, 03431, Phone: (800) 930-3367, Model PCP-100A.
4. Eric Jordan, Lockheed Martin Space Operations, Johnson Space Center/C71, Phone: (281) 483-6860.
5. Prodesco, P.O. Box 237, 700 West Park Avenue, Perkasie, PA, 18944, Phone: (215) 257-6566, <http://www.prodesco.com/aerospace.html>.

6. Materials Resources International, 811 West 5th Street, Unit 2, Lansdale, PA, 19446, Phone: (215) 631-7111.
7. "Slat Heater Boxes for Control of Thermal Environments in Thermal/Vacuum Testing", Eugene K. Ungar/JSC/EC2, SAE Technical Paper Series 1999-01-2135, 29th International Conferences on Environmental Systems (ICES), Denver, CO, July 12-15, 1999.
8. "Advanced Radiator Test Thermal Analysis", Gregg Weaver/LMSO/C70 and Kristin Stafford/LMSO/C70, MSAD-01-0265, April 5, 2001.
9. Stoyack, J.E., Cox, R.L., Smaltz, R.V., "Final Report, Option 1: Design and Development of a Flexible, Lightweight Radiator for an Inflatable Mars Spacecraft", Report prepared for NASA-Johnson Space Center, Contract Number NAS9-97207, Lockheed Martin Missiles & Fire Control, December 20, 2000.
10. Thermacore, Inc., 780 Eden Road, Lancaster, PA, 17604-3243, Phone: (717) 569-6551.
11. Minco Products, Inc., 7300 Commerce Lane, Minneapolis, MN, 55432-3177, Phone: (763) 571-3121.
12. "Advanced Radiator Concepts Thermal-Vacuum Test Detailed Test Procedure", Eric Jordan, CTSD-ADV-477, September 11, 2001.
13. Energy Science Laboratories, Inc., 6888 Nancy Ridge Drive, San Diego, CA, 92120-2232, Phone: (858) 552-2032.
14. “D684-10511-02 Thermal Control Subsystem Architecture Description Document, Volume 2, Revision G,” Boeing, January 4, 2000.
15. "Flexibility Test", David Westheimer/JSC/EC2, JSC CTSD TPS# 5M0120132, November 28, 2001.
16. ”DC-to-DC Converter Unit External Standard Interface Definition Document,”, SSP 30263:001, Revision D, NASA, Space Station Freedom Program Office, Reston, VA, May 1993.
17. “Enhanced Thermal Conductance of ORU Radiant Fin Thermal Interface using Carbon Brush Materials,” Christopher L. Seaman, Brett M. Ellman, and Timothy Knowles, Proceeding of Space Technology & Applications Forum (STAIF – 99), Albuquerque, NM, January 31 – February 4, 1999.

APPENDICES

APPENDIX A - ADDITIONAL INSTRUMENTATION FIGURES

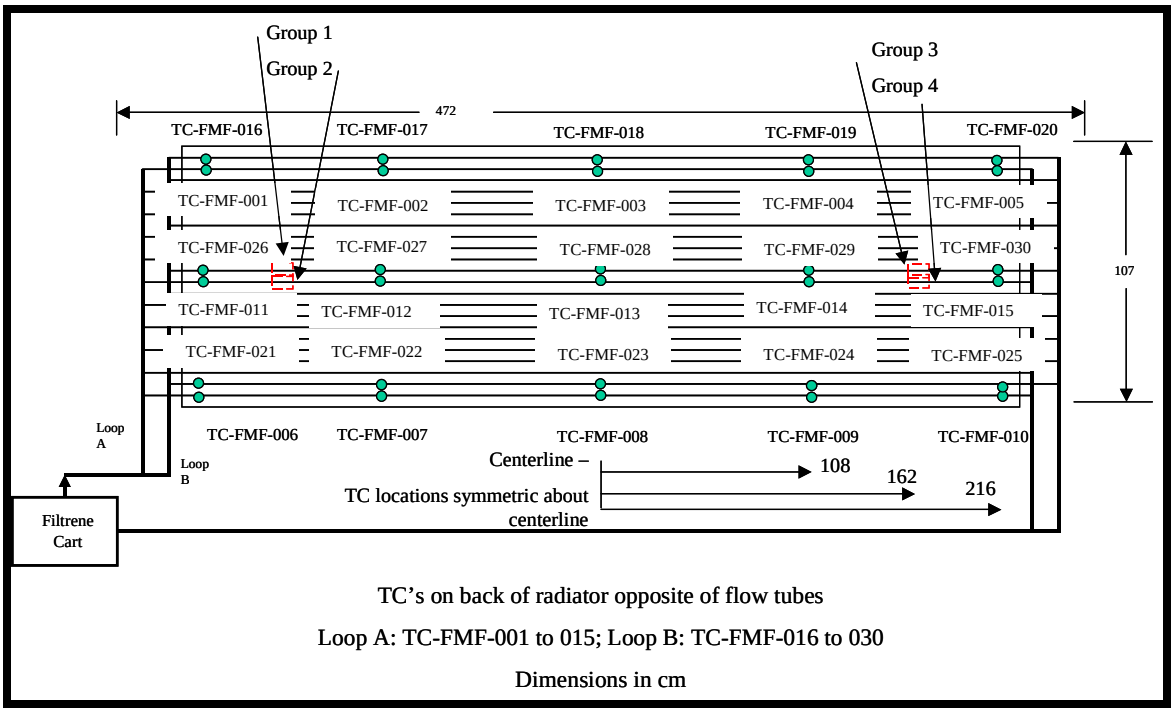

Figure 36 - FMF Instrumentation (2)

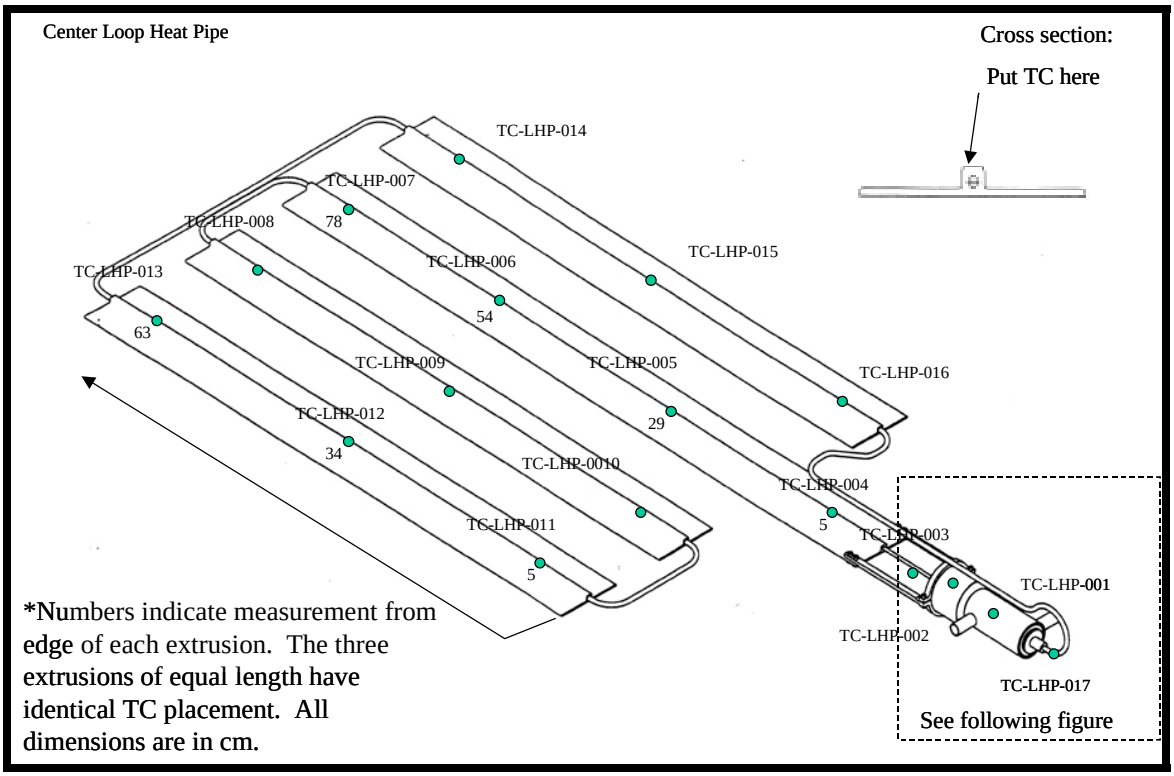

Figure 37 - LHP Instrumentation (2)

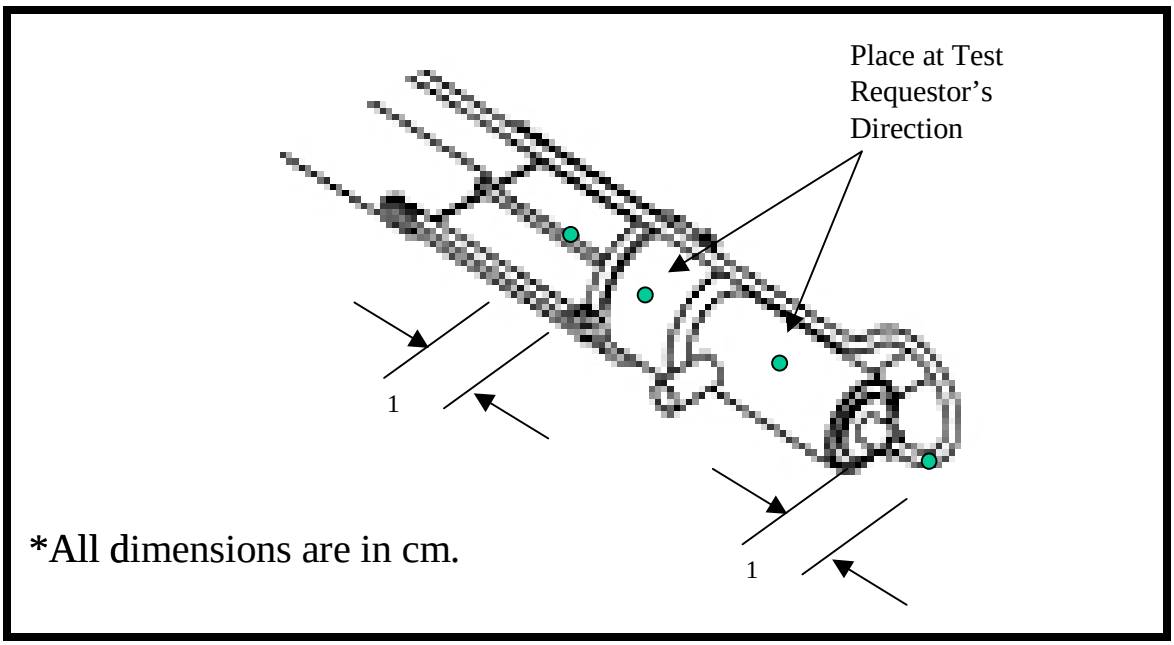

Figure 38 - LHP Instrumentation (3)

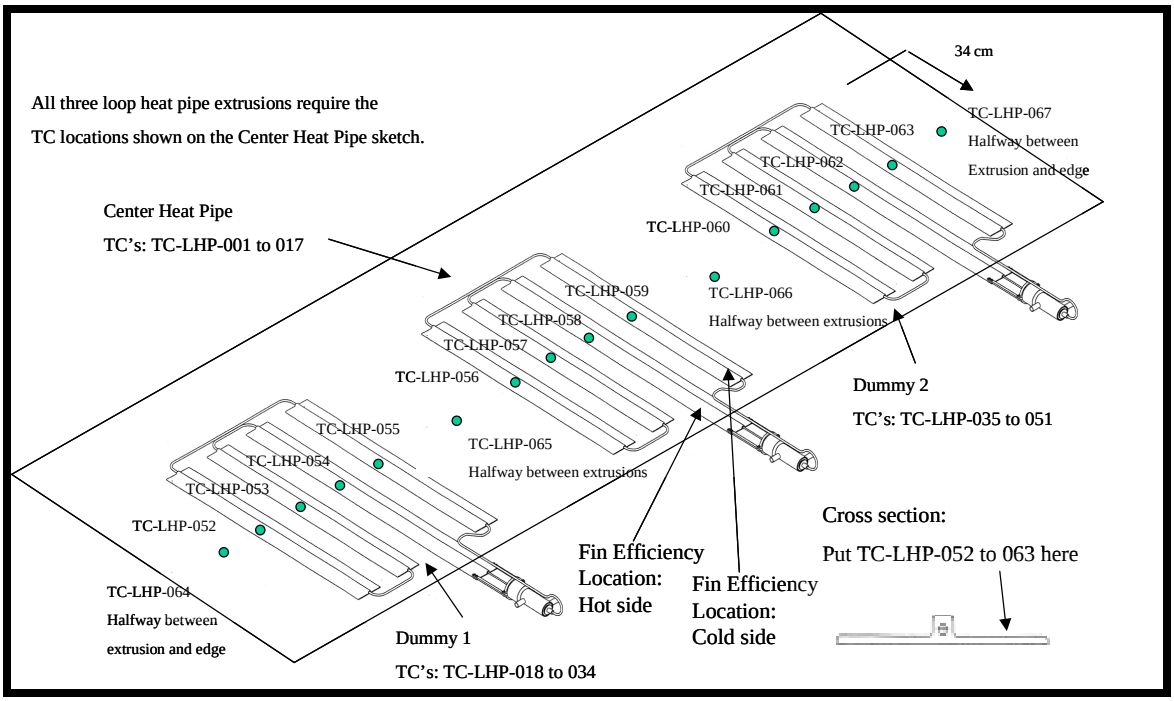

Figure 39 - LHP Instrumentation (4)

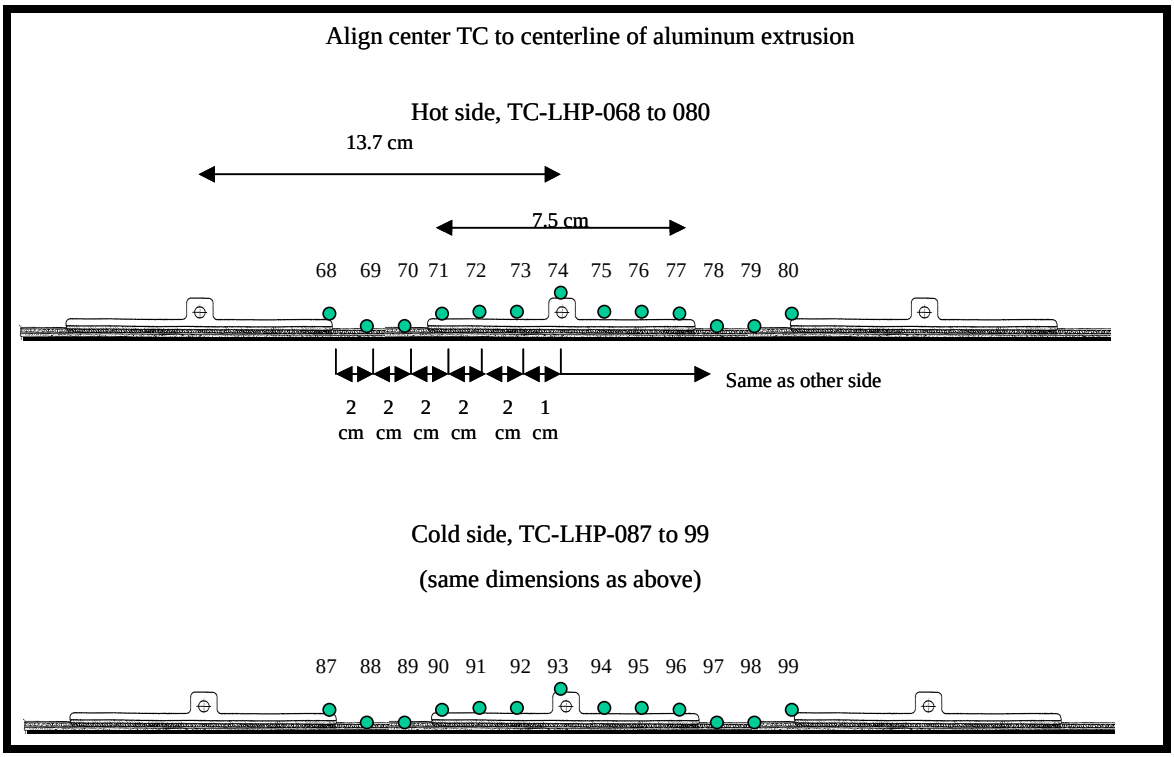

Figure 40 - LHP Instrumentation (5)

APPENDIX B - BASELINE TEST POINTS

Table 3 - Test Points for the FMF and LHP Radiators (as outlined in the DTP)

Case #	Environment Temp. (°F) ±10°F	Inlet Temperature (°F) ±5°F	Flow Rate (lb/hr) ±5 lb/hr
1	-240	100	50
2	-240	100	100
3	-240	100	250
4	-240	135	50
5	-240	135	100
6	-240	135	250
7	-240	135	500
8	-180	65	50
9	-180	65	100
10*	-180	65	50
11*	-180	65	100
12	-180	100	50
13	-180	100	100
14	-180	100	250
15	-180	135[9]	50
16	-180	135	100
17	-180	135	250
18	-180	135	500
19	-25.6	65	50
20*	-25.6	65	100
21*	-25.6	65	50
22	-25.6	65	100
23	-25.6	100	50
24	-25.6	100	100
25	-25.6	100	250
26	-25.6	135	50
27	-25.6	135	100
28	-25.6	135	250
29	-25.6	135	500
30	27	37	50
31	27	65	50
32	27	65	100
33	27	100	50
34	27	100	100
35	27	100	250
36	27	135	50

[*] This was a "single loop" or a "broken loop" test point, in which the effects of a "broken" loop were evaluated. For the FMF radiator, the flow in one of the loops was set to zero, and for the LHP radiator, the "dummy loop" heaters were turned off. Specifically, hand valve HV-1-02 was closed.

[9] The DTP actually stated 140°F. However, this was an error. The DTP should have read 135°F. When attempted in the actual test, the inlet temperature set point was 135°F.

Case #	Environment Temp. (°F) ±10°F	Inlet Temperature (°F) ±5°F	Flow Rate (lb/hr) ±5 lb/hr
37	27	135	100
38	27	135	250
39	27	135	500

Table 4 - Test Points for the Cold Plate (as outlined in the DTP)

Case #	Heater Power (Watts) ±20 W	Inlet Temperature (°F) ±5°F	Flow Rate (lb/hr) ±5 lb/hr
40[10]	694	39	125
41	694	63	125
42	1400	39	1100
43	2100	39	1100
44	2800	39	1100
45	3500	39	1100
46	4200	39	1100
47	4900	39	1100
48	5600	39	1100
49	1400	63	1100
50	2100	63	1100
51	2800	63	1100
52	3500	63	1100
53	4200	63	1100
54	4900	63	1100
55	5600	63	1100

[10] The DTP states, "Test points for the CVCP [carbon velvet cold plate] should follow the sequence shown....During test points 42-48 the heater power is increased incrementally until the Top Average Temperature reaches 100°F. The inlet temperature is then changed for test points 49-55 and the heater power is again increased incrementally until the Top Average Temperature reaches 100°F. Do not perform test points listed after this temperature is attained for that flow rate."

APPENDIX C - FINAL TEST POINTS

Table 5 - Amended FMF and LHP Radiator Test Points

Case #[11]	Environment Temp. (°F) ±10°F LHP/FMF	Inlet Temperature (°F) ±5°F LHP/FMF	Flow Rate (lb/hr) ±5 lb/hr	LHP Time Complete (GMT[12])	FMF Time Complete (GMT)
2	-105/-70	100	100	263-01:04	263-01:04
3	-105/-70	100	250	263-02:39	263-02:39
4	-105/-70	135	50	262-17:40	not complete
5	-105/-70	135	100	262-19:55	262-17:40
6	-105/-70	135	250	262-21:00	262-19:55
7	-105/-70	135	500	262-22:06	262-21:00
9	-65	65	100	266-12:04	266-10:01
10*	-65	65	50	266-16:43	not complete
11*	-65	65	100	266-14:33	not complete
12	-65	100	50	266-08:15	266-08:15
13	-65	100	100	263-09:48	263-09:12
14	-65	100	250	263-10:44	263-10:42
15	-65	135	50	263-15:00	263-15:00
16	-65	135	100	263-12:00	263-12:00
17	-65	135	250	263-13:00	263-13:00
18	-65	135	500	263-18:40	263-17:20
19	10	65	50	266-04:25	266-04:10
20*	10	65	100	263-23:28	264-01:15
21*	10	65/100	50	264-02:00	264-11:45
22	10	65/100	100	264-03:00	264-13:20
23	10	100	50	264-09:22	264-09:22
24	10	100	100	264-06:08	264-06:08
25	10	100	250	264-07:54	264-07:54
26	10	135	50	264-14:30	264-14:30
27	10	135	100	264-15:22	264-15:22
28	10	135	250	264-16:07	264-16:07
29	10	135	500	264-17:01	264-20:35
31	45	65	50	265-19:47	265-19:47
32	45	65	100	265-18:40	265-18:31
33	45	100	50	265-08:00	265-08:00
34	45	100	100	265-09:06	265-09:06
35	45	100	250	265-11:09	265-11:09
35.5	45	100	500	265-12:10	265-14:48
36	45	135	50	265-06:20	265-06:20

[11] Cases not listed (e.g., Case 1) were not completed during the test for either radiator.
[12] Greenwich Mean Time
[*] This was a "single loop" or a "broken loop" test point, in which the effects of a "broken" loop were evaluated. For the FMF radiator, the flow in one of the loops was set to zero, and for the LHP radiator, the "dummy loop" heaters were turned off. Specifically, hand valve HV-1-02 was closed.

Case #[11]	Environment Temp. (°F) ±10°F LHP/FMF	Inlet Temperature (°F) ±5°F LHP/FMF	Flow Rate (lb/hr) ±5 lb/hr	LHP Time Complete (GMT[12])	FMF Time Complete (GMT)
37	45	135	100	265-2:15	265-02:15
38	45	135	250	264-23:30	265-00:30
39	45	135	500	265-00:30	264-23:30

Table 6 - Amended Cold Plate Test Points

Case #	Heater Power (Watts) ±20 W	Inlet Temperature (°F) ±5°F	Flow Rate (lb/hr) ±5 lb/hr	Time Complete (GMT)
40	694	39	125	262-14:53
41	694	63	125	262-08:45
42	1400	39	1100	262-16:35
43	1000	39	1100	262-19:00
44	800	39	1100	262-20:30
45	780	39	1100	262-21:58
46	750	39	1100	262-23:15
47	680	39	1100	264-20:45
48	680	39	1100	265-14:53
49	100	63	1100	263-01:13
50	200	63	1100	263-02:32
51	400	63	1100	263-04:13
52	450	63	1100	263-05:19
53	694	63	1100	263-07:16
54	680	63	1100	264-18:00
55	680	63	1100	265-01:00

APPENDIX D - FMF RADIATOR TEST RESULTS

Table 7 - Detailed FMF Radiator Results

	Average Coupon Temperature (K)	Average Heat Rejection (m dot cP delta T, Watts) (assuming cp=0.827)	Total Heat Rejection (m dot cP delta T, Watts) (assuming cp=0.827) DISCOUNTING HEAT TRACE	FMF Avg Temps (TCs 1-30, K)	Calculated radiation heat transfer (Watts)	Uncertainty in the m dot cP delta T (Watts)	Uncertainty in the radiation heat transfer (Watts)
Case 2	230.90	701.90	1403.79	291.98	1228.28	±13.08	±18.24
Case 3	232.92	752.11	1504.22	297.41	1354.60	±17.88	±19.52
Case 5	239.75	851.74	1703.47	307.88	1576.80	±15.62	±22.15
Case 6	244.21	940.68	1881.36	315.00	1745.45	±20.46	±24.08
Case 7	245.98	955.52	1911.04	318.02	1822.83	±29.33	±24.94
Case 9	228.01	522.02	1044.05	277.11	886.45	±10.18	±15.12
Case 12	233.61	566.37	1132.74	285.47	1016.61	±10.07	±16.74
Case 13	231.54	687.43	1374.87	291.71	1212.04	±12.81	±18.16
Case 14	232.85	740.84	1481.69	297.56	1359.97	±17.71	±19.57
Case 15	233.56	721.83	1443.66	296.46	1317.97	±12.72	±19.30
Case 16	237.08	828.26	1656.53	305.50	1540.75	±15.10	±21.58
Case 17	241.57	933.33	1866.66	313.76	1744.67	±20.15	±23.83
Case 18	245.23	991.80	1983.61	318.14	1839.45	±29.75	±25.03
Case 19	251.40	350.92	701.84	279.16	576.92	±6.31	±16.08
Case 20	251.01	367.82	735.63	281.24	634.58	±8.00	±16.33
Case 21	251.69	343.08	686.16	279.35	576.39	±8.56	±16.14
Case 22	254.52	447.21	894.41	288.41	755.61	±11.47	±17.57
Case 23	257.50	462.50	925.01	292.97	824.46	±8.36	±18.43
Case 24	258.09	507.00	1013.99	295.90	896.27	±10.01	±18.97
Case 25	260.12	552.75	1105.51	300.69	998.22	±15.56	±19.94
Case 26	261.00	579.59	1159.18	303.56	1068.81	±10.34	±20.56
Case 27	264.53	674.38	1348.76	311.33	1248.42	±10.68	±22.35
Case 28	267.23	754.17	1508.34	317.14	1392.24	±17.83	±23.80
Case 29	268.89	795.99	1591.98	320.65	1483.11	±28.03	±24.73
Case 31	265.54	240.35	480.70	284.17	429.95	±4.81	±17.78
Case 32	266.21	271.63	543.25	286.20	468.24	±6.84	±18.05
Case 33	270.66	361.20	722.39	296.31	650.07	±6.72	±19.66
Case 34	271.43	407.57	815.14	299.43	724.60	±8.55	±20.16
Case 35	273.11	457.07	914.15	303.62	814.48	±14.56	±20.94
Case 35.5	274.14	484.37	968.74	306.77	890.47	±25.46	±21.54
Case 36	274.90	474.90	949.80	307.66	901.66	±8.57	±21.75
Case 37	277.79	569.72	1139.44	314.36	1057.74	±10.99	±23.18
Case 38	279.94	642.71	1285.42	319.84	1199.98	±16.45	±24.46
Case 39	280.52	676.63	1353.25	322.04	1266.55	±26.92	±25.00

Table 8 - Detailed FMF Radiator Results (2)

	Actual % Difference between Radiation and mdotcpDt	Average Measured Inlet Temp (deg F)	Average Measured Flow Rate per Loop (lbm/hr)	Average Delta P across Radiator (psi)	Loop A heat trace power that enters the inlet line downstream of the temperature probe but upstream of the radiator (Watts)	Loop B heat trace power that enters the inlet line downstream of the temperature probe but upstream of the radiator (Watts)	Heat Rejection from SINDA/FLUINT model (Watts)	FMF Heat Rejection per Area (Watts/m^2) mdotcpdt, discounting heat trace
Case 2	12.5%	98.4	101.32	6.26	0	0	1197	281.89
Case 3	9.9%	99.41	253.47	13.95	0	0	1280	302.05
Case 5	7.4%	131.7	108.63	3.88	0	0	1526	342.06
Case 6	7.2%	134.91	256.02	8.27	0	0	1646	377.78
Case 7	4.6%	134.52	499.26	17.77	0	0	1668	383.74
Case 9	15.1%	64.3	97.68	12.58	42	41.7	859	209.65
Case 12	10.3%	99.01	49.4	3.44	40.3	39.9	1038	227.46
Case 13	11.8%	97.67	99.24	6.3	0	0	1179	276.08
Case 14	8.2%	99.53	252.43	13.87	0	0	1287	297.53
Case 15	8.7%	128.06	52.38	2.82	0	0	1353	289.89
Case 16	7.0%	128.51	99.99	3.59	0	0	1495	332.64
Case 17	6.5%	132.92	249.18	8.09	0	0	1644	374.83
Case 18	7.3%	135.35	501.75	17.88	0	0	1690	398.32
Case 19	17.8%	67.63	50.91	6.01	41.9	41.6	579	140.93
Case 20	13.7%	64.27	100.35	11.8	0	0	617	147.72
Case 21	16.0%	95.42	51.66	6.31	0	0		137.78
Case 22	15.5%	100.82	102.68	7.57	0	0		179.60
Case 23	10.9%	100.84	51.25	3.57	0	0	825	185.74
Case 24	11.6%	96.68	100.35	5.78	0	0	875	203.61
Case 25	9.7%	99.22	253.61	13.43	0	0	952	221.99
Case 26	7.8%	127.42	52.37	2.19	0	0	1068	232.77
Case 27	7.4%	131.11	103.36	3.51	0	0	1215	270.84
Case 28	7.7%	133.78	251.09	7.82	0	0	1322	302.88
Case 29	6.8%	135.44	503.86	17.21	33.5	33.2	1362	319.67
Case 31	10.6%	69.51	50.17	4.59	41.2	40.8	425	96.53
Case 32	13.8%	68.19	102.84	9.47	40.8	40.5	455	109.09
Case 33	10.0%	98.86	51.42	2.24	38.7	38.4	643	145.06
Case 34	11.1%	98.29	100.3	4.66	38.2	37.9	708	163.68
Case 35	10.9%	101.09	252.15	11.93	37.5	37.3	777	183.56
Case 35.5	8.1%	104.7	495.88	24.29	36.8	36.5	829	194.53
Case 36	5.1%	127.23	51.54	1.09	36.5	36.2	887	190.72
Case 37	7.2%	132.18	100.92	2.37	34.8	34.5	1033	228.80
Case 38	6.6%	135.21	250.11	6.81	33.6	33.3	1138	258.12
Case 39	6.4%	135.42	500.18	16.77	33.4	33.1	1166	271.74

APPENDIX E - LHP RADIATOR TEST RESULTS

Table 9 - Detailed LHP Radiator Test Results

	Average Heat Input (m dot cP delta T, Watts) (assuming cp=0.827) Discounts Heat Trace	Desired Env. Temp (deg F)	Desired Env Temp (K)	Desired Inlet Temp. (deg F)	Desired Flow Rate (lb/hr)	Average Measured Environment Temp (K, using T to the 4th averaging)	Average Measured Inlet Temp (deg F) discounts heat trace	Average Measured Flow Rate (lbm/hr)	Average of Variac 1 (Watts)	Average of Variac 2 (Watts)	Average of Variac 3 (Watts)	Average of Variac 4 (Watts)
Case 2	-194.61	-105	197.04	100	100	197.97	99.80	102.61	59.23	60.00	68.60	59.29
Case 3	-737.31	-105	197.04	100	250	197.89	100.60	252.93	58.78	59.61	68.06	58.83
Case 4	77.22	-105	197.04	135	50	197.30	127.17	46.80	56.70	31.84	41.21	56.70
Case 5	-61.42	-105	197.04	135	100	199.14	133.43	100.03	56.48	57.25	65.59	56.31
Case 6	-622.16	-105	197.04	135	250	199.83	134.94	249.72	57.73	58.42	66.91	57.57
Case 7	-1422.56	-105	197.04	135	500	200.37	136.02	501.03	57.78	58.53	66.97	57.63
Case 9	38.81	-45	230.37	65	100	220.33	64.66	98.89	28.19	17.89	14.38	22.75
Case 10	53.20	-45	230.37	65	50	215.52	64.85	46.93	-0.64	0.65	0.33	0.41
Case 11	55.11	-45	230.37	65	100	216.61	64.51	101.45	-0.65	0.65	0.35	0.41
Case 12	92.73	-65	219.26	100	50	227.84	98.68	50.50	60.19	32.10	40.18	58.96
Case 13	46.73	-65	219.26	100	100	223.41	99.06	100.43	60.78	32.47	39.57	58.30
Case 14	-124.65	-65	219.26	100	250	223.59	100.93	251.79	60.88	32.56	39.62	58.53
Case 15	124.18	-65	219.26	135	50	224.88	127.35	49.13	59.08	31.78	38.57	56.69
Case 16	83.59	-65	219.26	135	100	224.65	129.67	99.20	60.01	32.09	39.13	57.53
Case 17	-41.71	-65	219.26	135	250	225.32	134.17	250.88	60.19	32.17	39.25	57.71
Case 18	-306.16	-65	219.26	135	500	226.12	135.77	501.31	60.01	32.33	39.16	57.57
Case 19	20.53	10	260.93	65	50	259.72	68.00	48.93	9.33	8.69	9.25	7.97
Case 20	25.15	10	260.93	65	100	261.03	64.39	97.10	60.81	32.78	39.64	58.68
Case 21	50.04	10	260.93	65	50	256.92	64.98	49.50	-0.56	0.73	0.47	0.50
Case 22	47.48	10	260.93	65	100	257.05	64.86	99.76	1.94	1.76	1.75	2.48
Case 23	82.74	10	260.93	100	50	262.92	100.91	50.48	56.14	30.65	40.06	58.57
Case 24	85.73	10	260.93	100	100	262.35	97.59	102.07	55.83	30.63	39.92	58.29
Case 25	85.76	10	260.93	100	250	262.81	99.90	251.91	56.11	30.58	40.03	58.57
Case 26	118.36	10	260.93	135	50	263.24	126.48	51.92	53.92	29.69	38.74	56.57
Case 27	118.06	10	260.93	135	100	263.66	131.37	101.17	53.48	29.52	38.50	56.15
Case 28	133.23	10	260.93	135	250	263.92	134.40	252.06	53.24	29.38	38.29	55.87
Case 29	153.68	10	260.93	135	500	263.93	133.67	498.21	53.26	29.40	38.31	55.82
Case 31	-12.54	45	280.37	65	50	275.33	69.45	51.43	8.80	8.27	8.81	7.59
Case 32	-28.07	45	280.37	65	100	275.38	67.86	104.15	8.80	8.28	8.87	7.61
Case 33	20.99	45	280.37	100	50	279.36	98.17	51.12	57.98	31.01	36.93	57.61
Case 34	24.66	45	280.37	100	100	279.44	98.29	99.79	58.07	31.08	36.96	57.64
Case 35	23.30	45	280.37	100	250	279.55	101.16	251.47	57.86	30.97	36.79	57.50
Case 35.5	20.98	45	280.37	100	500	279.41	101.68	499.58	56.91	30.48	36.24	56.57
Case 36	62.38	45	280.37	135	50	279.90	125.64	49.57	57.76	30.88	36.78	57.33
Case 37	82.07	45	280.37	135	100	280.06	132.29	100.48	57.62	30.88	36.80	57.01
Case 38	93.18	45	280.37	135	250	280.01	135.32	247.95	58.53	31.34	37.49	57.99
Case 39	109.86	45	280.37	135	500	280.18	136.62	499.32	57.90	31.09	37.06	57.50

Table 10 - Detailed LHP Radiator Test Results (2)

	Total of Variacs	LHP T to the 4th surface temp average (K)	Average radiation heat rejection (Watts)	Heat input to radiator (mdot plus variacs, Watts) discounts heat trace	Average radiation heat transfer per area (W/m^2)	Delta P (psi)
Case 2	247.12	285.6	418.40	52.51	261.3	0.49
Case 3	245.29	286.7	426.42	-492.02	266.3	1.25
Case 4	186.46	279.1	371.78	263.68	232.2	0.18
Case 5	235.63	289.8	447.60	174.21	279.6	0.32
Case 6	240.62	292.1	464.43	-381.54	290.1	0.93
Case 7	240.92	293.7	476.56	-1181.64	297.7	2.89
Case 9	83.20	262.7	196.71	122.01	122.9	0.91
Case 10	0.75	246.1	123.55	53.95	77.2	0.54
Case 11	0.75	247.8	128.19	55.86	80.1	0.94
Case 12	191.43	287.4	337.23	284.16	210.6	0.43
Case 13	191.11	284.6	332.38	237.84	207.6	0.49
Case 14	191.59	285.9	341.51	66.94	213.3	1.24
Case 15	186.12	288.1	353.54	310.30	220.8	0.23
Case 16	188.77	290.4	372.77	272.36	232.8	0.37
Case 17	189.33	292.8	389.69	147.62	243.4	0.96
Case 18	189.08	294.2	398.71	-117.08	249.0	2.94
Case 19	35.24	275.4	98.46	55.77	61.5	0.55
Case 20	191.91	295.5	243.76	217.06	152.3	0.78
Case 21	1.14	267.4	61.71	51.18	38.5	0.45
Case 22	7.93	267.9	64.14	55.41	40.1	0.78
Case 23	185.41	301.9	287.87	268.15	179.8	0.25
Case 24	184.67	301.1	284.73	270.40	177.8	0.50
Case 25	185.28	302.3	292.75	271.04	182.9	1.26
Case 26	178.91	304.6	311.07	297.27	194.3	0.24
Case 27	177.64	306.7	328.45	295.70	205.2	0.37
Case 28	176.78	308.0	338.50	310.01	211.4	0.97
Case 29	176.79	308.3	341.39	330.47	213.2	2.92
Case 31	33.47	284.1	63.05	20.93	39.4	0.56
Case 32	33.56	283.4	56.89	5.49	35.5	0.91
Case 33	183.53	310.5	261.56	204.52	163.4	0.41
Case 34	183.75	310.8	264.42	208.41	165.2	0.61
Case 35	183.11	311.6	271.28	206.41	169.4	1.39
Case 35.5	180.19	311.3	268.87	201.17	167.9	3.54
Case 36	182.76	314.3	296.16	245.14	185.0	0.34
Case 37	182.31	315.9	311.30	264.38	194.4	0.49
Case 38	185.34	316.9	321.55	278.52	200.8	1.10
Case 39	183.54	317.5	326.96	293.40	204.2	3.10

APPENDIX F - CARBON VELVET COLD PLATE TEST RESULTS

These are the data required to determine the heat load applied and removed from the Carbon Velvet Cold Plate.

Table 11 - Carbon Velvet Cold Plate Results

Test Point	FM-CP-1, COLD PLATE INLET FLOWRATE (lbm/hr)	HT-CP-1 COLD PLATE INLET LINE TEMP (°F)	HT-CP-2 COLD PLATE OUTLET LINE TEMP (°F)	cp (kJ/kg*K)	Q (W) mdot*cp* (Tout -Tin)	uncertainty (±W)	Adjusted Heater Power (W)
41	128.08	63.68	89.22	3.40	780.63	4.60	695.86
40	124.67	43.58	72.04	3.37	837.47	4.49	685.33
42	1106.62	40.90	47.75	3.34	1775.95	36.84	1399.49
43	1101.27	40.89	47.56	3.34	1723.19	36.66	1015.52
44	1098.59	40.95	45.96	3.34	1289.62	36.48	806.37
45	1099.17	40.87	45.15	3.34	1100.52	36.47	779.57
46	1096.22	40.83	44.68	3.34	988.24	36.35	753.68
49	1104.80	63.90	64.44	3.38	142.55	37.02	108.54
50	1106.12	63.91	64.65	3.38	194.61	37.07	209.13
51	1107.02	63.90	65.37	3.38	384.94	37.11	396.64
52	1103.52	63.93	65.43	3.38	392.20	37.00	452.95
53	1103.91	63.93	66.87	3.38	768.70	37.05	693.26
54	1108.80	64.22	66.99	3.38	728.07	37.22	666.17
47	1099.25	41.50	43.66	3.34	557.06	36.41	664.24
48	1095.29	39.46	41.89	3.33	623.20	36.25	659.91
55	1100.36	63.98	66.80	3.38	736.23	36.93	664.03

These are the time-averaged surface mounted thermocouple readings for each Carbon Velvet Cold Plate test point.

Table 12 - Temperatures, Top Surface Top Set of Radiant Fins

Test Point	TC 01 (°F)	TC 02 (°F)	TC 03 (°F)	TC 04 (°F)	TC 05 (°F)	TC 06 (°F)	TC 07 (°F)	TC 08 (°F)	TC 09 (°F)
40	117.49	117.05	119.44	117.70	118.31	117.55	110.26	108.10	114.68
41	132.52	132.17	134.20	132.41	133.05	132.19	125.08	122.89	129.30
42	152.08	152.90	156.69	153.27	155.41	154.43	142.79	139.78	148.68
43	126.38	126.68	130.30	127.05	128.45	127.74	118.51	115.94	123.78
44	110.77	110.68	113.76	111.21	112.20	111.50	103.29	100.97	108.16
45	108.17	108.04	111.00	108.58	109.51	108.79	100.57	98.18	105.29
46	106.04	105.85	108.74	106.40	107.26	106.53	98.45	96.05	103.10
47	99.05	98.53	101.30	99.27	99.86	99.26	91.72	89.69	96.44
48	96.03	95.40	98.23	96.24	96.72	96.07	88.42	86.30	93.18
49	72.77	71.40	72.72	72.30	71.67	71.17	67.13	66.32	70.65
50	80.52	79.34	80.82	80.15	79.77	79.21	74.31	73.00	77.83
51	96.97	96.05	97.97	96.80	96.81	96.16	89.98	88.18	93.88
52	101.67	100.82	102.84	101.52	101.65	100.97	94.52	92.63	98.53
53	121.55	121.07	123.61	121.71	122.33	121.59	113.71	111.48	118.28
54	120.61	120.03	122.63	120.80	121.28	120.60	113.16	111.20	117.74
55	119.49	118.95	121.53	119.70	120.23	119.48	111.88	109.89	116.52

Table 13 - Temperatures, Between Fins of Top Set of Radiant Fins

Test Point	TC 10 (°F)	TC 11 (°F)	TC 12 (°F)	TC 13 (°F)	TC 14 (°F)	TC 15 (°F)	TC 16 (°F)	TC 17 (°F)	TC 18 (°F)
40	104.38	114.57	114.20	113.69	111.02	103.84	110.47	111.89	113.99
41	120.31	166.38	129.38	128.37	126.08	119.66	125.40	127.11	128.94
42	127.92	147.24	147.49	145.61	141.11	127.14	141.57	143.80	147.06
43	106.97	122.16	122.37	121.04	117.82	106.86	117.99	118.75	122.36
44	94.68	106.92	107.01	106.30	103.69	94.57	103.24	103.96	107.05
45	92.65	104.52	104.57	103.92	101.35	92.50	100.73	101.48	104.41
46	90.93	102.49	102.48	101.87	99.38	90.76	98.64	99.41	102.28
47	85.49	95.64	95.58	95.09	92.56	85.14	92.01	93.00	95.58
48	82.70	92.60	92.45	92.02	89.45	82.13	88.85	89.81	92.36
49	69.55	71.11	71.18	70.98	70.58	69.57	68.54	69.86	70.45
50	75.87	78.90	78.75	78.61	77.78	75.77	75.79	77.12	77.92
51	88.90	229.25	94.46	94.38	92.70	88.67	91.10	92.39	93.79
52	92.59	190.56	98.93	98.83	96.94	92.31	95.51	96.79	98.34
53	108.15	118.30	118.15	117.69	115.39	107.86	114.11	115.44	117.68
54	107.38	117.28	117.09	116.59	114.45	106.98	113.44	114.68	116.95
55	106.55	116.27	116.06	115.70	113.16	106.20	112.25	113.51	115.78

Table 14 - Temperatures, Between Fins of Bottom Set of Radiant Fins

Test Point	TC 19 (°F)	TC 20 (°F)	TC 21 (°F)	TC 22 (°F)	TC 23 (°F)	TC 24 (°F)	TC 25 (°F)	TC 26 (°F)	TC 27 (°F)
40	93.59	94.88	91.09	88.56	89.41	88.76	80.06	93.62	82.69
41	109.39	110.82	106.94	105.07	105.70	105.30	96.38	109.48	99.38
42	106.08	108.57	101.79	97.38	99.26	96.19	90.51	108.54	87.21
43	91.62	93.39	88.00	84.07	85.53	83.38	76.52	92.50	75.83
44	82.39	83.85	79.32	75.83	77.00	75.53	67.88	82.51	68.79
45	80.66	82.14	77.73	74.36	75.50	74.19	66.19	80.72	67.48
46	79.33	80.77	76.50	73.18	74.29	73.07	64.92	79.30	66.46
47	75.60	76.88	73.02	70.13	70.94	70.05	62.03	75.38	63.90
48	72.78	74.20	70.25	67.48	68.29	67.60	59.36	72.64	61.22
49	69.18	69.82	68.38	67.22	67.30	68.56	56.88	66.39	64.70
50	73.61	74.44	72.54	71.20	71.41	72.39	60.85	71.20	67.99
51	83.26	84.38	81.51	79.71	80.14	80.47	69.76	81.63	75.20
52	86.05	87.23	84.12	82.14	82.63	82.79	72.30	84.61	77.29
53	97.83	99.44	95.21	92.57	93.41	92.72	83.36	97.32	86.27
54	97.81	99.19	95.23	92.46	93.19	92.43	83.79	97.19	86.33
55	97.00	98.58	94.51	91.94	92.68	92.08	83.14	96.52	85.84

Table 15 - Temperatures, Cold Plate

Test Point	TC 28 (°F)	TC 29 (°F)	TC 30 (°F)	TC 31 (°F)	TC 32 (°F)	TC 33 (°F)	TC 34 (°F)	TC 35 (°F)	TC 36 (°F)
40	83.11	79.54	78.58	81.84	81.31	78.60	81.65	79.63	78.67
41	98.07	94.16	93.67	96.92	96.11	93.64	96.76	94.42	93.61
42	84.01	79.72	75.68	83.21	81.56	75.92	83.01	79.77	76.07
43	76.23	72.22	69.51	74.65	73.94	69.67	74.54	72.19	69.82
44	70.15	66.37	64.52	68.54	68.08	64.61	68.40	66.36	64.72
45	67.94	64.32	62.65	66.89	66.05	62.71	66.52	64.37	62.80
46	66.85	63.27	61.72	65.84	65.01	61.78	65.49	63.33	61.87
47	66.14	62.58	61.35	64.58	64.34	61.39	64.38	62.63	61.42
48	61.97	58.60	57.61	61.03	60.52	57.59	60.71	58.68	57.56
49	67.58	64.67	66.33	66.27	66.38	66.15	65.98	64.85	66.14
50	69.46	66.62	67.90	68.56	68.38	67.74	68.27	66.83	67.71
51	75.36	72.32	72.72	74.91	74.11	72.61	74.41	72.52	72.60
52	77.58	74.44	74.58	77.00	76.22	74.50	76.54	74.62	74.49
53	85.32	81.94	80.97	84.86	83.76	80.97	84.40	82.07	80.98
54	88.96	85.19	84.13	87.15	86.96	84.17	86.94	85.22	84.19
55	86.13	82.65	81.85	85.23	84.58	81.84	84.93	82.80	81.82